VILNIUS UNIVERSITY

INGRIDA ANTONOVA

CORTICAL DYNAMICS OF VISUOSPATIAL PROCESSING INVESTIGATED BY EEG MICROSTATES METHOD

Doctoral Dissertation

Biomedical Sciences, Biophysics (02B)

Vilnius, 2016

Disertation prepared in 2011 – 2016 at Vilnius University and the University Hospital of Psychiatry, University of Bern

Scientific supervisors:
Prof. dr. Thomas Koenig (University of Bern, University Hospital of Psychiatry, Biomedical Sciences, biophysics – 02B) (2013-10-14 – 2016-03-31)

Dr. Kastytis Dapšys (Vilnius University, Biomedical Sciences, biophysics – 02B) (2011-10-01 – 2013-10-13)

Scientific consultant:
Doc. dr. Inga Griškova-Bulanova (Vilnius University, Biomedical Sciences, biophysics – 02B)

VILNIAUS UNIVERSITETAS

INGRIDA ANTONOVA

SU REGIMUOJU ERDVĖS SUVOKIMU SUSIJUSIO SMEGENŲ AKTYVUMO DINAMIKOS TYRIMAS EEG MIKROBŪSENŲ METODU

Daktaro disertacija

Biomedicinos mokslai, Biofizika (02B)

Vilnius, 2016 metai

Disertacija parengta 2011 – 2016 metais Vilniaus universitete ir Universitetinėje psichiatrijos ligoninėje, Berno universitete

Moksliniai vadovai:
Prof. dr. Thomas Koenig (Berno universitetas, Universitetinė psichiatrijos ligoninė, biomedicinos mokslai, biofizika – 02B) (nuo 2013-10-14 iki – 2016-03-31)

Dr. Kastytis Dapšys (Vilniaus universitetas, biomedicinos mokslai, biofizika – 02B) (nuo 2011-10-01 iki 2013-10-13)

Mokslinė konsultantė:
Doc. dr. Inga Griškova-Bulanova (Vilniaus universitetas, biomedicinos mokslai, biofizika – 02B)

Table of Contents

The materials presented in this dissertation are published in:

1. Antonova I, Bänninger A, Direks T, Griškova-Bulanova I, Koenig T, Kohler A (2015) Differential recruitment of brain networks during visuospatial and color processing: Evidence from ERP microstates. Neuroscience 305:128-138

2. Antonova I, van Swam C, Hubl D, Dierks T, Griskova-Bulanova I, Koenig T (2016) Reaction time in a visual 4-choice reaction time task: ERP effects of motor preparation, and hemispheric involvement. Brain Topography, doi: 10.1007/s10548-016-0473-7

Abbreviations

Ag/AgCl – silver/silver-chloride

ANOVA – analysis of variance

AUC – area under the curve

BOLD – blood-oxygenation-level-dependent

EEG – electroencephalography

EOG – electrooculography

ERP – event-related potential

CRT – choice reaction time

DTI – diffusion tensor imaging

fMRI – functional magnetic resonance imaging

fNIRS – functional near-infrared spectroscopy

GFP – global field power

IPL – inferior parietal lobule

LL – left lateral

LRP – lateralized readiness potential

ML – left medial

MR – right medial

RR – right lateral

RT – reaction time

rTMS – repetitive transcranial magnetic stimulation

SPL – superior parietal lobule

SRT – simple reaction time

TANCOVA – topographic analysis of covariance

TANOVA – topographic analysis of variance

TCT – topographic consistency test

tDCS – transcranial direct current stimulation

TMS – transcranial magnetic stimulation

1. Introduction

Visuospatial information plays an important role in interaction with the environment. Visuospatial processing includes the processing of information about objects and/or location in space (Hannay et al. 1976; McIntosh et al. 1994) and information about relations between the objects parts in space (Benton et al. 1975; Benwell et al. 2014; de Graaf et al. 2010). The analysis of relations between object parts in space is called visuospatial judgment, and is considered a higher order function of visuospatial processing (de Graaf et al. 2010). The examples of relations between object parts in space are spatial features such as like line orientation (Benton et al. 1975), angles (de Graaf et al. 2010), or distances (Benwell et al. 2014).

The brain areas involved in visuospatial judgment are well-known, as is the superiority of the right hemisphere in visuospatial processing (de Graaf et al. 2010; Lehmann et al. 2006; Sack et al. 2002a; Vannini et al. 2004, 2007, 2008). These findings were revealed by functional magnetic resonance imaging (fMRI) – a method that provides high spatial resolution, i.e. helps visualize the brain areas activated during the execution of a particular task. However, the temporal resolution of fMRI is low and temporal dynamics of networks activation during visuospatial processing are yet to be resolved.

In order to investigate the temporal dynamics of visuospatial processing, it is advisable to use electroencephalography (EEG) – a method with good temporal resolution. When a task is executed during an EEG recording, event-related potentials (ERPs) can be obtained. An ERP is a brain's response to a particular event. An EEG signal can be analysed by using various techniques, microstates being one of them.

Microstates are transient stable EEG topographies that can be assigned to a particular ERP based on latency and topography (Michel et al. 2009). Microstate analysis has an advantage over classical ERP analysis in that it allows one to explore the activation of cortical networks by precisely

quantifying the different features of the temporal dynamics, such as onset, duration or strength, between different conditions and groups. Microstate analysis enables one not only to assess the temporal dynamics, but also to compare findings with the ones obtained in imaging studies.

Microstate analysis is a valuable tool, but it has never been used to investigate visuospatial processing, thus such a study would add new knowledge of temporal dynamics to the existing findings. Changes in the activation of different brain areas are observed when visuospatial processing is impaired (Prvulovic et al. 2002; Thulborn et al. 2000; Vannini et al. 2007, 2008; White et al. 2011), therefore EEG-based investigations of visuospatial processing could contribute to the development of easy and widely available screening procedures aimed at detecting and investigating the impairment of visuospatial processing.

1.1. Aim and objectives

The aim of this work was to investigate the temporal dynamics of visuospatial information processing by means of EEG microstate analysis.

The objectives were as follows:

1. To compare the dynamics of visuospatial processing during the visuospatial and color judgment task.

2. To evaluate the effects of stimulus lateralization on the temporal dynamics of visuospatial processing during the location judgment task.

1.2. Novelty and relevance

This is the first time when the visuospatial judgment and color judgment paradigm has been used in an EEG study and differences in the

temporal dynamics of visuospatial and non-spatial judgment have been observed.

This is the first time when a task with four lateralized stimuli has been applied in an EEG study to investigate visuospatial processing and differences in the temporal dynamics have been observed in response to differently lateralized visual stimuli.

1.3. Practical applications

The findings provide new information about the temporal dynamics of visuospatial processing. The paradigms used in these studies have been verified as suitable for EEG studies, while microstate analysis is a particularly sensitive tool that can be used to depict temporal dynamic and their differences between conditions. This is important for the future clinical studies, as well as for the development of EEG-based screening procedures intended to evaluate the impairment of visuospatial processing.

1.4. Statements to be defended

1. Visuospatial judgment and non-spatial color judgment differ in temporal dynamics of the EEG microstates.

2. Lateralized visual stimulation evokes early lateralized EEG microstates that represent early lateralized N1 topographically and by latency.

2. Literature review

2.1. Visuospatial processing

The processing of visuospatial information is considered to be crucial for effective interaction with the environment. Visuospatial processing can be defined as the processing and interpretation of visual information about the location of objects in space. The higher-order functions of visuospatial processing are also important. One example of higher-order visuospatial processing is visuospatial judgment, which allows one to analyze subtler spatial relations and features of visual images, such as angles and distances (de Graaf et al. 2010). Another higher-order function of visuospatial processing is visual-motor integration. It is important for the effective coordination of movements in accordance with incoming visual information and thus allows us to perform activities such as reaching objects, reading and writing (e.g. Barnhardt et al. 2005; Daly et al. 2003).

The first scientific explanation of visuopatial cognition was suggested by Descartes in his Treatise of Man (1662), where he proposed his theory of a "natural geometry" and reflected on the problem of the processes taking place in the brain during the perception of distance (Marshall and Fink 2001). Since then, numerous studies have been conducted to investigate different aspects of visuospatial perception. Visual streams (Ungerleider and Mishkin 1982), hemispheric dominance and areas important for visuospatial processing (Weintraub and Mesulam 1987) were revealed while studing brain damaged patients. With the emergence of lesion studies and, more recently, with the appearance of functional brain imaging techniques, it became possible to investigate the neural networks and anatomical substrates involved in visuospatial information processing. Thus, more precise findings were reported regarding brain activation during visuospatial processing (de Graaf et al. 2010; Vannini et al. 2004).

2.1.1. Visual streams

Based on the findings of the brain lesion studies, it was proposed that there are distinct pathways for different visual information – in other words that there are two distinct visual systems in the brain, both projecting from the primary visual cortex (see **Figure 2.1**): a projection to the posterior parietal cortex was defined as a dorsal "Where" stream that processes spatial information, and the ventral "What" stream that projects to the inferotemportal cortex and processes information about objects (see Mishkin et al. 1983; Ungerleider and Mishkin 1982). Later, the existence of two streams in the visual system was confirmed by using functional neuroimaging techniques (Haxby et al. 1991; McIntosh et al. 1994; Shen et al. 1999).

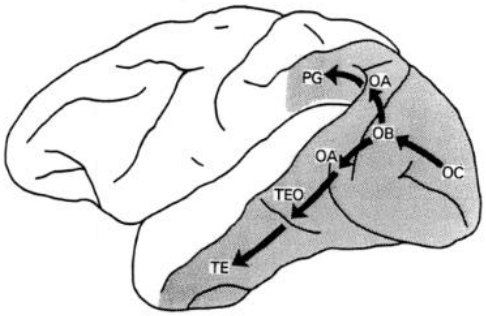

Figure 2.1. The two cortical visual streams. Each pathway is depicted schematically by arrows that begin in the primary visual cortex (OC) and diverge within the prestriatal cortex (OB and OA). The dorsal stream ("Where") courses into the parietal cortex (PG) and is crucial for spatial vision; the ventral pathway ("What") courses into the temporal cortex (TEO and TE) and is crucial for object vision. (From Mishkin et al. 1983)

More recently, the dorsal stream has been relabeled as the "How" stream due to its role in transforming visual information in preparation for direct action (Goodale and Milner 1992; Creem and Proffitt 2001). However, the two streams ("What" and "How") cannot be strictly separated, as these two pathways are functionally dependent due to the extent of inter-stream interactions (Schenk and McIntosh 2010). Moreover, Creem and Proffitt (2001) proposed in their review that, since "How" and "Where" streams are involved in visuospatial processing, they could be functionally and structurally distinguished within the parietal cortex, and that this was preferable to

relabelling “Where” as “How”. This view was later supported by Rizzolatti and Matelli (2003), who argued that the dorsal stream, along with the parietal cortex, forms two functionally distinct streams. A more recent study suggested that the dorsal sream should be divided into the three functionally and anatomically distinct pathways, all of which are involved in visuospatial processing (Kravitz et al. 2011).

Studies of the streams in the visual system revealed the brain areas involved in visuospatial processing. Thus, today it is well known that the human parietal cortex is activated during the performance of visuospatial tasks (review by Creem and Proffitt 2001; Haxby et al. 1991; McIntosh et al. 1994; Newcombe et al. 1987; review by Rizzolatti and Matelli 2003; Shen et al. 1999). However, as Culham and Kanwisher (2001) pointed out in their review, the investigation of the human parietal cortex presents a significant challenge because it encompasses a large anatomical area, which includes both somatosensory regions and regions that belong to the functional category of “association cortex” and are characterized by rather complex, multimodal responses. The numerous studies carried out in humans and monkeys studies demonstrated that the parietal lobes are activated during a variety of tasks involving both spatial and non-spatial functions such as visuomotor control, attention, eye movements, spatial and non-spatial working memory, mental imagery, task switching, and other (Culham and Kanwisher 2001; Husain and Nachev 2007).

2.1.2. Hemispheric asymmetry

Numerous studies of different neurodevelopmental disorders such as schizophrenia (Bilder et al. 1994; Crow et al. 2013; Løberg et al. 1999; Sharma et al. 1999), autism (Herbert et al. 2002, 2005; Lo et al. 2011) and dyslexia (Heim et al. 2003a, 2003b; Jenner et al. 1999; Spironelli et al. 2008) reported altered or reduced hemispheric asymmetries in structure, function or connectivity. For instance, in schizophrenia, altered performance asymmetries

in visuospatial processing tasks (Ribolsi et al. 2013) and a lack of normal asymmetries in the occipito-parietal areas (Bilder et al. 1994; Sharma et al. 1999) were observed.

It is well known that the two hemispheres of the brain are not fully symmetrical and differ in their structure and function. Ocklenburg and Güntürkün (2012) reviewed different studies in animals and humans and pointed that hemispheric functional lateralization likely was inherited from common ancestors. In different species, this hemispheric specialization is maintained by asymmetrical connections. The human brain is not the only one characterized by hemispheric asymmetry; indeed, the same peculiarity is found in the other species and is important for normal brain functioning. Thus, several explanations were proposed for the phenomenon. Ringo et al. (1994) suggested that functional lateralization makes information processing faster, since there is no need to spend any extra time to transfer information to another hemisphere and thus to delay processing. More recently, Rogers et al. (2004) reported that cerebral lateralization enhances the efficiency of information processing when two different cognitive tasks have to be executed simultaneously.

Traditionally, hemispheric asymmetry have been observed and defined as asymmetry in behaviour, structure, function, and connectivity.

Behavioural lateralization is the most prominent when it comes to handedness (Amunts et al. 2000; Corballis 2014; Tommasi 2008). Other types of asymmetry in the brain can be related to handedness to a different extent, as this is discussed below.

Anatomical asymmetry was observed as various structural differences between two homotopic regions of the two hemispheres at a macroscopic level, including hemispheric protrusion and petalia (see Toga and Thompson 2003) and asymmetries in the central sulcus (Amunts et al. 2000) (both more prominent in right handed men) or differences in volume (Penhune et al. 1996), as well as at a microscopic level (Jenner et al. 1999).

Functional asymmetries were observed as local functional properties that differ between the left and right sides of the brain and result in hemispheric specialization (Gazzaniga 2000; Stephan et al. 2003). Calosotomised (or "split brain") patients demonstrated a strict dichotomy in hemispheric specialization, in that the left hemisphere was responsible for language processing (Gazzaniga 2000; Sperry 1968) whereas the right hemispheric was responsible for visuospatial processing (Corballis et al. 1999, 2002; Funnell et al. 1999; Sperry 1968). However, Corballis (2003) argued that the strict dichotomy between language and visuospatial processing is oversimplified and that the hemispheric asymmetries are likely to arise at higher levels of visual processing, so that the right hemisphere can be described as more "visually intelligent" than the left hemisphere. In 2002, Han and colleagues reported that the right hemisphere is dominant during the processing of global visuospatial, while the left hemisphere is more active in analyzing local visuospatial information.

The differences between the two hemispheres are not limited to their structure and functions. Intra- and inter-hemispheric connectivity is also characterized by structural and functional asymmetry (Büchel et al. 2004; Lo et al. 2011; McIntosh et al. 1994; Nielsen et al. 2013; Salvador et al. 2005; Stephan et al. 2007; Toga and Thompson 2003). The first attempts to measure differences in inter- and intra-hemispheric connectivity were made in 1994. McIntosh et al. (1994) found rightward hemispheric asymmetries for face matching and visouspatial processing tasks, along with stronger right-to-left interhemispheric connections. Asymmetrical white matter tracts were found in different studies (Büchel et al. 2004; Lo et al. 2011; Nielsen et al. 2013). These findings support the hypothesis that the left hemisphere is dominant in linguisting information processing, while the right hemispheric specializes in visuospatial processing.

To summarize, inter-hemispheric differences in structure, functions, and connections are important for maintaining hemispheric asymmetry and specialization. Hemispheric specialization is an important mechanism that

helps enhance the processing of particular information and is essential for normal brain functioning. New studies using paradigms of visuospatial processing with centrally presented and lateralized stimuli could reveal correlates between visuospatial impairment and changes in hemispheric asymmetry, for example, in schizophrenia.

2.1.3. Corpus callosum and interhemispheric transfer time

In the visual system, the right and left visual hemifields are represented in different cerebral hemispheres. The hemispheres are connected together by the corpus callosum. Besides, the splenium of the corpus callosum connects the visual areas of the brain (Bocci et al. 2014; Catani et al. 2003; Gazzaniga 2000). Thus, the splenium allows the visual information that has reached one hemisphere to be transferred to the other (contralateral) hemisphere. This interhemispheric transfer takes more time due to indirect pathways and can be measured by performing simple tasks.

In 1912, Poffenberger proposed a tool to assess the interhemispheric information transfer. Poffenberger suggested applying a simple reaction time (SRT) task with lateralized visual stimuli: Stimuli are presented either to the left or to the right visual field while the responses are given with the hand that is either ipsilateral (uncrossed condition) or contralateral (crossed condition) to the side being stimulated (see Poffenberger 1912; and a review by Marzi 1999). Uncrossed responses are those provided with the hand that is ipsilateral to the lateralized visual stimulation. They do not require interhemispheric transfer, because a response originates in the same hemisphere as the one activated by visual stimulation, so reaction time is shorter. In case of crossed responses, the visual information reaches one hemisphere, but the response hand is controlled by the contralateral hemisphere, therefore the interhemispheric transmission of information is required and this results in an increased reaction time.

Until now, the Poffenberger paradigm has been used in different studies in order to evaluate information transmission from one hemisphere to another both in healthy subjects (Ipata et al. 1997; Mooshagian et al. 2008; Saron and Davidson 1989; Westerhausen et al. 2006; Whitford et al. 2011), and in patients with callosal abnormalities (Aglioti et al. 1993; Mooshagian et al. 2009) or disturbancies such as callosotomy (Aglioti et al. 1993; Iacoboni et al. 1994; Iacoboni and Zaidel 1995; Mooshagian et al. 2009).

It was shown that the corpus callosum makes an important contributions to the execution of responses to visual stimuli. Patients with complete callosal agenesis or total section of the corpus callosum had a great differences in reaction time between crossed and uncrossed responses, with substantially longer reaction times for crossed responses (Aglioti et al. 1993; Iacoboni and Zaidel 1995), while in the cases of partial callosotomy reaction times were shorter and differences between crossed and uncrossed responses were smaller (Iacoboni et al. 1994; Iacoboni and Zaidel 1995).

It was also demonstrated that response times can be modulated by spatial attention, so that reaction times to crossed responses decrease (Mooshagian et al. 2008). Several studies reported that interhemispheric transfer can be measured by analysing the latencies of early ERPs (Ipata et al. 1997; Saron and Davidson 1989; Westerhausen et al. 2006; Whitford et al. 2011). The authors found shorter latencies of the P1 and the N1 for the direct pathway (uncrossed conditions). Diffusion tensor imaging (DTI) findings showed that interhemispheric transfer time correlates with structural properties of the corpus callosum (Westerhausen et al. 2006).

Interhemispheric transmission differs depending on the direction of the information flow. Interhemispheric transfer from the left (visually stimulated) to the right (motor response generation) hemisphere was found to be significantly shorter (Westerhausen et al. 2006). Simultaneously, differences in reaction times were found for crossed responses produced with left and right hands. The following explanations were suggested. On the one hand, this asymmetry occurs due to the superiority of the right hemisphere in detecting

visual stimuli, and is reflected in the advantage of the left visual field over the right. On the other hand, the advantage of the right hand over the left can be explained by a superiority of the left hemisphere for the movements planning (meta-analysis of Marzi et al. 1991; meta-analysis of Bisiacchi et al. 1994; Whitford et al. 2011). Despite this asymmetry, the interhemispheric transfer through the splenium allows one hemisphere to compensate the deficits of the other (Bocci et al. 2014). However, aberrations of the splenium can contribute to visual deficits, while callosal intersection or absence of the corpus callosum leads to prolonged interhemispheric transfer times as well as visual dysfunctions (Bocci et al. 2014).

2.1.4. Parietal cortex and hemispheric involvement in visuospatial processing

The evidence of hemispheric involvement and the importance of the parietal cortex in visuospatial processing was gained from two main groups of studies: lesion studies and imaging studies.

The evidence from lesion studies was obtained after the investigation of actual lesions and lesions induced by temporal transcranial magnetic stimulation (TMS). Patients who suffer from brain lesions or have undergone a calosotomy have participated in different studies for decades. Visuospatial processing was more impaired if the lesion was in the right hemisphere (review Mesulam 1999). Hemispatial neglect or hemineglect is a common neuropsychological condition observed after damage to the contralateral hemisphere (Mesulam 1999). It is defined by a profound lack of awareness of information obtained from the contralesional side of the environment or body. This inability to process visual information is caused by a lateralized disruption of spatial attention (but not due to a lack of sensation) (Mesulam 1999; Smania et al. 1998).

Impaired visual localization was observed in right hemisphere damaged patients (Hannay et al. 1976; Smania et al. 1998; Tartaglione et al. 1981).

Tartaglione et al. (1981) reported that patients with right hemisphere brain damage suffered from greater visuospatial impairment than patients with a lesion of the left hemisphere; however, a reduction of accuracy in the visual field contralateral to the lesion was found in both hemispheric groups of patients. In addition, left hemineglect caused progressively slower responses to stimuli situated not only on the left but also on the right (Bartolomeo and Chokron 1999). Mesulam (1981) suggested that the left hemisphere attends to contralateral visual field while the right hemisphere is responsible for both visual fields, so that the neglect stemming from a lesion of the right hemisphere is more severe.

In their study of brain-damaged patients, Weintraub and Mesulam (1987) found that in right-handed subjects hemineglect was more frequent and severe after damage to the right as opposed to the left parietal cortex. However, studies of left-handed patients with unilateral brain damage have yielded contradictory results. Left-handed patients with a damaged left hemisphere performed normally but left-handers with damage of the right hemisphere had visuospatial deficits (Masure and Benton 1983). In contrast, another study reported that left-handers exhibit hemispheric asymmetry opposite to the one observed in right-handers, i.e. the left hemisphere is superior in the visuospatial task and the right hemisphere is superior in the verbal task (Marzi et al. 1988).

Benton et al. (1975, 1978) reported that patients who had lesion in the right hemisphere exhibited a highly impaired performance in the visuospatial Judgment of Line Orientation task, compared to healthy subjects or patients with a lesion in the left hemisphere. Thus, the authors proposed using this task to investigate unilateral brain lesions. One of the studies found that patients' performance of the Judgment of Line Orientation task was significantly impaired after they sustained damage either to the right or to the left parietal lobe, but more severe impairment was associated with right parietal damage (Ng et al. 2000). One of the more recent studies reported that the impaired execution of this task was associated with lesions in the right posterior parietal lobule (Tranel et al. 2009). The line bisection task revealed significant left

hemineglect caused by damage to the right posterior cortex (Reuter-Lorenz and Posner 1990).

Smania et al. (1998) found that damage to the right hemisphere caused left hemineglect, while damage to the left hemisphere had no effect on visual attention (Smania et al. 1998). More recently, it was reported that right parietal damage caused bilateral deficits in transient visual attention (Battelli et al. 2003). Visuospatial processing deficits can accompany lesions in different locations of the right parietal cortex. The findings based on patients with a damaged right hemisphere showed that the inferior parietal sulcus plays a role in endogenous attentional control, whereas lesions in the middle inferior parietal sulcus result in neglect (Vandenberghe et al. 2005). Furthemore, hemispatial neglect can be caused by a lesion in the right inferior parietal lobule, which not only plays a crucial role in spatial processing but also has non-spatial functions related to attention (Husain and Nachev 2007). More recently, "virtual lesions" in the parietal cortex induced by rTMS were shown to produce an extinction of visual stimuli in the visual field contralateral to the lesion that was similar to neglect, especially after a right parietal "lesion" (Hilgetag et al. 2001). It was shown that the intraparietal sulcus is involved in visuosptatial processing bilaterally, but only rTMS to the right parietal lobe impaired the ability to perform the visuospatial task (Sack et al. 2002b).

Imaging studies revealed precise parietal areas involved in different aspects of visuospatial processing. It was shown that imaginary objects containing spatial information (clocks) induce bilateral activity in the posterior parietal cortex even in the absence of visual stimulation (Formisano et al. 2002; Trojano et al. 2000). Schicke et al. (2006) compared ERPs and blood-oxygenation-level-dependent (BOLD) signals to both imagined and actual stimuli, and found similar paterns of activation in the posterior parietal regions (the inferior and superior parietal lobules).

Studies of visuospatial judgment pointed to the posterior parietal cortex (de Graaf et al. 2009) and, more specifically, to the superior and inferior parietal lobules (Fink et al. 2000; Lehmann et al. 2006; Prvulovic et al. 2002;

Sack et al. 2002a; Sack et al. 2002b; Vannini et al. 2004) as the main areas involved in visuospatial judgment. It was found that the right parietal cortex is involved in different aspects of visuospatial processing (Colby and Goldberg 1999, Mesulam 1999), and is responsible not only for visuospatial judgment, but also for visuospatial attention (Hilgetag et al. 2001; Müri et al. 2002; Shulman et al. 2010) and for learning various combinations of visual feature (Roser et al. 2011). Within the parietal cortex, different regions are responsible for different processes: A region of the lateral superior parietal cortex is activated by the spatial location task (Haxby et al. 1991) and Judgment of Line Orientation task (Ng et al. 2000). The inferior parietal cortex is involved in attentional processes (Husain and Nachev 2007; Vandenberghe et al. 2005). Intraparietal sulcus is activated during visuospatial judgment both either actual or imagined stimuli (Formisano et al. 2002; Sack et al. 2002b).

The outcome of all these studies regarding visuospatial processing was the assumption that the right hemisphere is dominant and the parietal cortex plays a crucial role in visuospatial perception. It is important to mention that the right hemisphere is capable to compensate for the disfunction of the left hemisphere, because it can attend to both the left and the right visual fields, while the left hemisphere can only deal with the visual information coming from the contralateral visual field (Fink et al. 1997; Formisano et al. 2002; Mesulam 1981, 1999; Nobre et al. 1997; Sack et al. 2002b, 2005; Sheremata et al. 2010; Weintraub and Mesulam 1987).

2.1.5. Visuospatial processing dysfunction

A particular variety of visuospatial processing dysfunction was observed in Huntington's desease: visuospatial recognition memory and spatial working memory (visuospatial processing capacity) were affected while visuospatial judgment remained relatively intact (Mohr et al. 1991). Similarly, Dierks et al. (1999) reported that performance of Huntington's patient in the visuospatial task was similar to healthy control with only one exception –

namely, prolonged RTs; however, extensive atrophy was observed in the parietal areas.

Impaired visuospatial skills were observed as one of the early symptoms in Alzheimer's disease (Arnáiz and Almkvist 2003; Thulborn et al. 2000). Thulborn et al. (2000) reported a reduction in right parietal activation and increased activation of the left intraparietal sulcus. The authors suggested that this alternation of the normal asymmetry may reflect the progressive dysfunction in spatial attention associated with Alzheimer's disease. Vannini et al. (2007) also found a stronger activation of the left parietal lobule in Alzheimer's disease in contrast to the stronger activation of the right parietal lobule in controls. Other studies also associated visuospatial processing dysfunction with atrophy of the superior parietal lobule. However, the authors found that this parietal (or dorsal stream) dysfunction can be compensated by recruiting the ventral stream (Prvulovic et al. 2002; Vannini et al. 2008).

Among other symptoms, different visuospatial perception deficits are seen in schizophrenic patients. Several studies associated these deficits with a dysfunction of the parietal cortex (McCourt et al. 2008; Ribolsi et al. 2013; White et al. 2011). For instance, a load dependent decrease in parietal lobe activation was observed during the visuospatial working memory task (White et al. 2011). Moreover, the authors reported that temporal cortex activation increased along with the memory task load. Schizophrenic patients and their first degree relatives demonstrated a lack of rightward pseudoneglect as an indicator of reduced visuospatial lateralization to the right hemisphere (Ribolsi et al. 2013). The authors hypothesized that these results could be caused by a specific impairment in the functioning of the right parietal cortex. Disruptions in the functioning of the right hemisphere were not the only phenomenon observed in schizophrenia; so were changes in callosal integration, which were correlated with the abnormalities in visuospatial processing connected to the disorder (McCourt et al. 2008).

2.2. Visuospatial judgment and areas involved in visuospatial judgment

Visuospatial judgment tasks are those concerned with features such as distances (Benwell et al. 2014; Fink et al. 2000, 2003; Foxe et al. 2003; Reuter-Lorenz and Posner 1990; Ribolsi et al. 2013; Waberski et al. 2008), line direction (Benton et al. 1975, 1978; Hardoy et al. 2004; Lindgren and Benton 1980; Ng et al. 2000; Ska et al. 1990; Tranel et al. 2009) or angles (de Graaf et al. 2009, 2010; Sack et al. 2002a, 2002b, 2007; Lehmann et al. 2006; Vannini et al. 2004, 2008).

In line direction task, refered to as the Judgment of Line Orientation task, participants have to determine a degree of line orientation (that is, match two lines). A number of studies showed that the right parietal cortex is important for the successful execution of this task (Benton et al. 1975, 1978; Ng et al. 2000; Tranel et al. 2009). However, most of the studies that employed the Judgment of Line Orientation task involved patients with brain lesions (Benton et al. 1975, 1978; Ng et al. 2000; Tranel et al. 2009) or were limited to behavioural experiments (Benton et al. 1975, 1978; Hardoy et al. 2004; Ska et al. 1990). The findings of a more recent fMRI study revealed strong activation of the superior parietal lobe and thus supported the importance of the parietal cortex in visuospatial judgment (Ng et al. 2000).

Another paradigm frequently used in visuospatial processing studies is the line bisection task (Reuter-Lorenz and Posner 1990; Fink et al. 2000, 2003; Benwell et al. 2014). Participants have to mark middle of a line manually (Ribolsi et al. 2013) or are presented with a mark and have to decide whether it is located in the middle (Fink et al. 2000, 2003; Waberski et al. 2008). The line bisection task is used to examine unilateral neglect (Reuter-Lorenz and Posner 1990) or pseudoneglect (Benwell et al. 2014; Ribolsi et al. 2013). The fMRI studies found that the execution of the line bisection task was associated with stronger activity in the right posterior parietal cortex (more specifically, in the superior posterior and inferior parietal lobe) (Fink et al. 2000, 2003). ERP and source localization findings pointed to the same structures, largely those

situated in the right hemisphere: the superior posterior parietal cortex and the inferior posterior parietal cortex (Waberski et al. 2008). Ribolsi et al. (2013) reported that the line bisection performance of schizophrenic patients was partially corrected by selective right posterior parietal transcranial direct current stimulation (tDCS). Through manipulating the length of the lines, the researches demonstrated that greated perceived length evoked stronger right parieto-occipital responses around the latency of the N1 component (Benwell et al. 2014; Foxe et al. 2003). The authors suggested that the increased N1 may reflect a stronger attentional response to longer lines.

One more paradigm used to assess angles is known as the "Clock task". These tasks activate dorsal stream and parietal cortex. The "Clock task" has an advantage compared to other two paradigms in that it is possible to use different modifications to measure the changes in visuospatial processing that depend on task difficulty, and this concerns RT as well as the correctness or accuracy of the performance.

Different versions of the "Clock task" were used in previous studies (de Graaf et al. 2009, 2010; Sack et al. 2002a, 2002b, 2007; Lehmann et al. 2006; Vannini et al. 2004, 2008). One of these versions consists of two conditions or tasks. The first assignment is a non-spatial color task ("Color") where the size of the angle has to be ignored. The second is a visuospatial-judgment condition where only the angle have to be assessed while the color has to be ignored ("Angle") (de Graaf et al. 2009, 2010; Sack et al. 2002a, 2002b, 2007). The other version of the "Clock task" is visuospatial judgment task, with modifications to enhance task difficulty, i.e. different length of the clock hands (Lehmann et al. 2006; Prvulovic et al. 2002; Vannini et al. 2004, 2007, 2008).

Sack et al. (2002a) used the "Clock task" to address the question of parietal cortex functionality by applying repetitive transcranial magnetic stimulation (rTMS) over the parietal cortex. The authors were able to demonstrate that the superior parietal lobule is functionally important for the execution of the "Clock task", where the subjects had to discriminate angles, colors (control task), or a conjunction of both. A combined functional magnetic

resonance imaging (fMRI), TMS and behavioral study (Sack et al. 2007) revealed that both angle and color judgment tasks increased neuronal activity in parietal and frontal regions of the two hemispheres. In this particular study, TMS was applied to both the right and the left superior parietal lobules, but only right parietal TMS resulted in a significantly increased RT in the angle but not the color task performance.

In addition, Sack et al. (2007) found that functional connectivity between right superior parietal lobule (SPL), right postcentral gyrus and right middle frontal gyrus was enhanced during the execution of the visuospatial judgment task. Subsequent studies (de Graaf et al. 2009, 2010) applied TMS and fMRI methods to investigate effective connectivity between the posterior parietal cortex and the middle/inferior frontal cortex and thus test the extent to which these areas contribute to visuospatial judgment. The authors found that the fMRI effective connectivity directed influence from frontal to parietal cortex, but the timing of TMS effects was similar for both parietal and frontal sites.

Regarding networks activation, both the "Angle" and the "Color" tasks activated overlapping areas (de Graaf et al. 2010; Sack et al. 2002a). The authors reported that significant differences in the strength of activation were found only in areas were more specific to the performance of a certain task (visuospatial or non-spatial).

In another sequence of investigations, the "Clock task" with different difficulty levels was used (Lehmann et al. 2006; Prvulovic et al. 2002; Vannini et al. 2004, 2007, 2008). The task difficulty was a modulating factor of cortical activity during visuospatial judgment. Different levels of difficulty were achieved by changing the length of clock hands (Vannini et al. 2004).

Vannini et al. (2004) applied event-related fMRI to measure the BOLD signal and the spatial extent of the activation to increasing task difficulty. They found that activation in the right and left superior parietal lobules increased as the level of the task difficulty increased. RT correlated with task difficulty (Lehmann et al. 2006; Vannini et al. 2008). Thus, in other study (Lehmann et

al. 2006), single-trial reaction-time-dependent hemodynamic response predictors were used to investigate differences in brain activation regarding RT and task difficulty. As with the previous study, the authors found the activation of the superior and inferior parietal lobules. Moreover, they observed that, as task difficulty increased, other brain regions were also involved in the execution of visuospatial judgment, i.e. the networks involved bilateral caudate nucleus, insula, right inferior frontal gyrus, and left precentral gyrus.

Furthemore, the differences in brain activation during visuospatial judgment were investigated between healthy subjects and Alzheimer's disease patients (Prvulovic et al. 2002; Vannini et al. 2008). In both groups, the overlapping neural networks were engaged in visuospatial judgment. As the task difficulty increased, the Alzheimer's patients showed less or no activation in several network regions, which was interpreted as failure to modulate neural response to increased difficulty of the task. Interestingly, possible compensatory mechanisms were observed in Alzheimer's disease patients, such as the stronger activation of the left parietal lobule (Vannini et al. 2007) and the recruitment of the ventral stream (Prvulovic et al. 2002; Vannini et al. 2008) during the execution of visuospatial judgment task. The involvement of the ventral stream increased with the task difficulty.

2.3. Reaction time: An index of efficiency

Reaction time (RT) is the simple behavioural measure of time from the onset of the stimulus to the response, and is used to quantify the speed of reaction. RT experiments started in the middle of the 19th century (Donders 1969; Nicolas 1997). Donders (1969) showed that RT can be used to study mental chonometry – that is, the stages of information processing and the speed of mental processes. Since then RT has been considered to be an index of processing speed and is the major dependent variable in different behavioural experiments.

RT is used to investigate behavioural responses and is considered to be an important index of the efficiency of information processing. It can reflect the dominance of the hemisphere during the performance of a particular task (e.g. Bestelmeyer and Carey 2004; Frecska et al. 2004) or point at a dysfunction of the hemisphere (Frecska et al. 2004; Matsuda et al. 2011).

RT varies between individuals and between responses of the same person. This variability was accounted for by age (Dykiert et al. 2012; Hultsch et al. 2002; Tamnes et al. 2012), fluctuations of brain activity (Ramchurn et al. 2014), and white matter properties, such as volume (Walhovd and Fjell 2007), density, diameter and myelinisation of the axons (Madsen et al. 2011; Tuch et al. 2005).

2.3.1. Reaction time tasks: SRT and CRT

RT and accuracy of responses are the main parameters used to measure the efficiency of task execution in any behavioural experiments. RT is the measure of the speed of information processing.

RT can be investigated by applying different paradigms. One of them, referred to as the Poffenberger paradigm (1912), has already been discussed above.

The other tasks used to investigate RT are simple reaction time (SRT) and choice reaction time (CRT) tasks. These two tasks differ in the number of possible stimuli and responses: In the SRT task, there is only one stimulus and one response. In the CRT task, several stimuli can appear and the response must correspond to the stimulus. SRT tasks allow one to investigate differences in the speed of sensory processing. The findings of SRT studies show RT differences related to stimulus modality (e.g. Kalyanshetti and Vastard 2013; Shelton and Kumar 2010) and the subject's handedness (Annett and Annett 1979; Kalyanshetti and Vastard 2013), as well as differences between individuals (Annett and Annett 1979) and genders (Shelton and Kumar 2010),. In contrast, CRT tasks are used to investigate the speed of cognitive

processing: stimulus discrimination, response selection and attention (Bestelmeyer and Carey 2004; Frecska et al. 2004; Fu et al. 2010; Heinze et al. 1990; Johannes et al. 1995; Luck et al. 1990; Mangun and Hillyard 1991; Nobre et al. 1997; Störmer et al. 2009).

When it comes to CRT tasks, Posner-type paradigms with different cues (Posner 1980) are often applied to investigate lateralized stimulation and attention. The cueing paradigms use central or endogenous cues that point to the location of upcoming stimulus and thus direct the subject's attention to the left or right from the fixation point (Frecska et al. 2004; Mangun and Hillyard 1991; Nobre et al. 1997). Peripheral or exogenous cues appear at the same side or the same location as the upcoming stimulus and direct the subject's attention to that particular location (Fu et al. 2010). Cross-modal cueing can also be used (Bestelmeyer and Carey 2004; Störmer et al. 2009). Other types of paradigms do not use cueing but participants are required to direct their attention either to the left or to the right side (Heinze et al. 1990; Johannes et al. 1995; Luck et al. 1990). Both types of cueing induce attentional shifts and may have an impact on RT.

CRT experiments without the strong involvement of attentional networks use no cue and no instructions to pay attention to a particular side of stimulation (Matsuda et al. 2011; Ramchurn et al. 2014; Tuch et al. 2005). The findings of these studies show how RT differs between visual fields (Matsuda et al. 2011; Ramchurn et al. 2014; Tuch et al. 2005) and response hands (Ramchurn et al. 2014; Tuch et al. 2005). Using this method, the differences in RT to lateralized stimuli were found between healthy subjects and schizophrenia patients (Matsuda et al. 2011).

2.3.2. Reaction time, handedness and hemispheric dominance

Numerous studies investigated hand dominance in SRT or CRT task performance and hemispheric asymmetry regarding handedness. However, these studies have reported contradictory findings. These findings were

interpreted as the effect of hemispheric dominance during the execution of a particular task.

Right hand preference is more common than left hand preference, and it may be assumed that the right hand ought to be faster, at least in right-handers, due to left hemisphere dominance regarding movements. This was confirmed in two studies where right-handers demonstrated faster right hand responses in SRT (Kalyanshetti and Vastrad 2013) and CRT task (Steel et al. 2002) performance.

Schlutter et al. (1998) showed that the left hemisphere is dominant for movement selection in both right- and left-handed subjects. The authors carried out the SRT and CRT task study with transcranial magnetic stimulation (TMS) over the premotor cortex. In this study, TMS stimulation of the left premotor cortex resulted in the prolonged RTs for both right and left hand responses. Similarly, TMS stimulation over the left primary motor cortex also increased RT, but only in left-handed subjects. In right-handed subjects, no such hemispheric difference was found and RT was slower after TMS over either the left or the right primary motor cortices (Basso et al. 2006).

However, the findings of several other studies were conflicting. Annett and Annett (1979) applied a 2-CRT task with lateralized visual stimuli and observed faster right hand responses in a minority of the subjects, while the majority exhibited the faster left hand responses. These differences were not related to the dominant hand. Likewise, another CRT study reported faster left hand responses to lateralized visual stimuli (Barthelemy and Boulinguez 2001). Besides, left hand responses were faster than right hand responses in a SRT (visual detection) task and classical pointing task, and this was interpreted as the right hemisphere dominance in visuospatial processing in manual aiming asymmetries, as well as in movement planning (Barthelemy and Boulinguez 2001). In cued CRT tasks, the superiority of the left hand supported right hemisphere dominance (Bestelmeyer and Carey 2004; Frecska et al. 2004). Nobre et al. (1997) reported that almost of the right-handed participants had faster RTs for stimuli presented in the right visual field; however, a minority of

the subjects exibited the opposite effect or no differences. Despite the differences in RT between visual fields, the posterior parietal cortex was activated predominantly in the right hemisphere. However, cueing is known to activate visuospatial attentional networks, thus the left hand superiority could be accounted for by the right hemisphere dominance in visual spatial information processing and visual attention (Konrad et al. 2009; Thiebaut de Schotten et al. 2011; Tuch et al. 2005). On the other hand, cueing is not necessary to achieve stronger activate right hemisphere: Tuch et al. (2005) applied CRT task with lateralized visual stimuli and found that faster RT were correlated with white matter tracts relevant to visuospatial processing predominantly in the right hemisphere.

2.3.3. Intraindividual and interindividual variability of reaction time

RT shows intraindividual trial-by-trial and interindividual variability.

Interindividual RT variability originates from variability in white matter and its properties (Madsen et al. 2011; Tuch et al. 2005; Walhovd and Fjell 2007). Furthermore, a negative correlation was found between the variance in individual RT and the volume of white matter and cortical gray matter: RT variability increased as the volume decreased (Walhovd and Fjell 2007). However, the underlying neural mechanisms for this variability are not yet fully clear since the other possible causes remain unknown.

Diffusion tensor imaging (DTI) techniques are frequently used to investigate correlates between the white matter pathways and RT. The findings of these studies have allowed researchers to link RT variability to white matter pathways and to describe the white matter pathways and their asymmetry according to their diffusion parameters (Konrad et al. 2009; Madden et al. 2004; Madsen et al. 2011; Tuch et al. 2005; Walhovd and Fjell 2007). Correlations between RT and measured white matter structural properties were observed for white matter tracts of attentional brain networks such as the

parieto-frontal network, predominantly in the right hemisphere (Konrad et al. 2009, Thiebaut de Schotten et al. 2011).

Moreover, interindividual RT variability was related to resting-state (brain activity at rest then no task has to be performed) network topology. Zhou et al. (2012) found that increased functional connectivity in the alpha and gamma bands correlated with a longer RT. Thus, the authors hypothesised that RT is related to the efficiency with which information is integrated across distributed brain regions.

On the within subjects level, intra-individual variability in reaction time is considered to be an index of central nervous system functioning and age related differences (Dykiert et al. 2012). Increased RT variability correlates with poorer performance in cognitive tasks in older adults (Hultsch et al. 2002). In children, this variability decreases when white matter integrity increases (Tamnes et al. 2012). Ramchurn et al. (2014) reported that trial-to-trial RT variability has its ERP correlates: the shorter RTs can be predicted by the higher P300 amplitude.

2.4. EEG

Electroencephalography (EEG) is a non-invasive method used to register brain activity. Proposed by H. Berger in 1929, it was one of the first methods to investigate brain activity (see review by Kaiser 2005).

EEG measures the electric field produced by the neuronal activity. EEG signal originates from sources deeper in the brain. To be more precise, the generators of EEG signal are the postsynaptic potentials of the pyramidal neurons (reviewed by Olejniczak 2006). These electrical signals go through the brain tissues, skull and scalp and can then be registered on the surface of the scalp. Afterwards the electrical field is recorded from the electrodes attached to the scalp.

EEG is a valuable tool for investigating brain activity during the performance of different tasks, because it has high temporal resolution (ms)

compared to other methods – fMRI (s) or functional near-infrared spectroscopy (fNIRS) (100 ms). An example of an EEG recording is shown in **Figure 2.2**. Due to the high temporal resolution, EEG is used in different studies to investigate neuronal temporal dynamics during the execution of particular tasks (e.g. Mangun and Hillyard 1991; Saville et al. 2011; Wascher et al. 2009). The various EEG components of sensory and cognitive information processing – event related potentials (ERP) – were described (Di Russo et al. 2002; Friedman 1984; Fu et al. 2010; Mangun and Hillyard 1991; Ramchurn et al. 2014; Roth et al. 1978; Saville et al. 2011; Wascher et al. 2009).

The EEG/ERP method has certain limitations: a poor spatial resolution, the necessity to filter the signal from the noise and to average signal from many trials in order to extract the ERP signal from the EEG. However, due to the advantage in temporal resolution, easy application and relatively low costs, the EEG technique is very important in clinical practice.

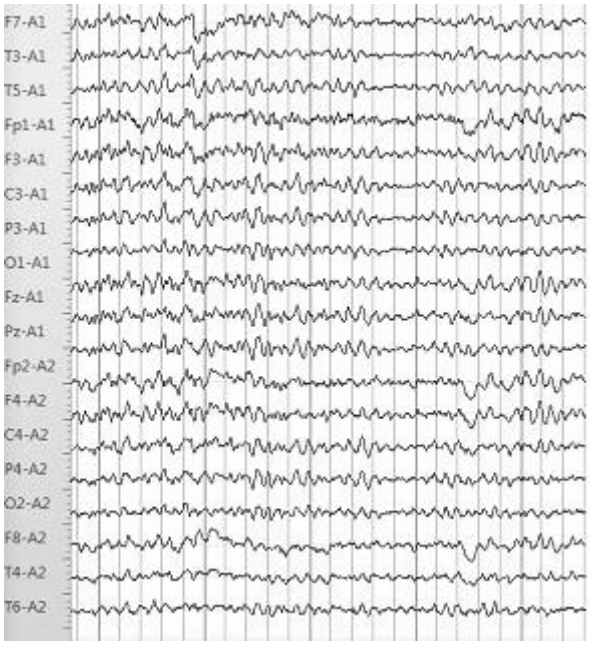

Figure 2.2. An example of an EEG recording.

2.5. ERPs

An ERP or event-related potential is a very small voltage brain response to a specific event or stimulus (Sur and Sinha 2009). ERPs are measured by

means of EEG, because they cannot be seen in a single trial EEG due to their low voltage in comparison to the voltage the EEG waveforms (Coles and Rugg 1996). After averaging, ERPs are observed as a series of voltage fluctuations. These fluctuations form the complex ERP waveform, so that a single ERP component can be defined as one of the component waves of this complex waveform (Woodman 2010). Due to the voltage fluctuations, a peak of the component wave can be either positive (P) or negative (N); the wave can also be named after its latency or an order in the complex. Thus, ERP components are usually labelled P1, N1, P2, etc. P1, N1, P3 and the other main visual components are shown in **Figure 2.3**. As Woodman (2010) concluded, ERPs are well-suited for revealing aspects of perceptual, attentional and cognitive processes that are unobservable with behavioral methods alone.

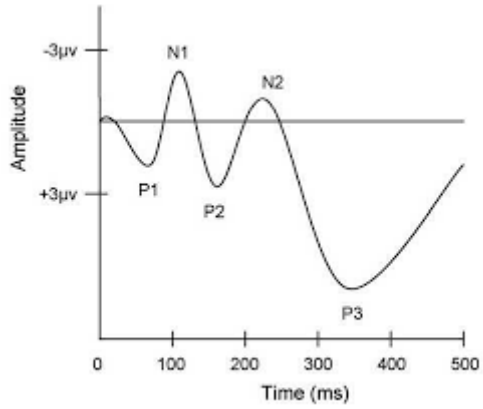

Figure 2.3. The main components of visual event related potentials.

2.5.1. P1

The P1 is an early ERP component and usually appears 80 - 130 ms after stimulus onset (Hillyard and Kutas 1983; Johannes et al. 1995). The amplitude of the P1 is larger contralaterally to the stimulation side (Hillyard and Anllo-Vento 1998; Liu et al. 2009). It is known that the P1 reflects the sensory processing of incoming information and can be modulated by selective spatial attention (Fu et al. 2010; Heinze et al. 1990; Hillyard and Anllo-Vento 1998; Johannes et al. 1995; Luck et al. 1990; Mangun and Hillyard 1991;

Störmer et al. 2009). Besides, it can be sensitive to different features of the stimuli (Johannes et al. 1995; Michel et al. 1992). Murray et al. (2001) used lateralized stimuli and observed different brain activation patterns related to visual stimulation, but found no systematic relationship between peak P1 latency and SRT.

2.5.2. N1

The second important early visual component is the N1. The latency of the N1 usually has a peak 140 - 200 ms after the stimulus onset (Hillyard and Anllo-Vento 1998; Hillyard and Kutas 1983; Johannes et al. 1995). The N1 shows the increased amplitude contralaterally to the stimulation side (Hillyard and Anllo-Vento 1998; Mangun and Hillyard 1991; Wascher et al. 2009), and can be modulated by features of the stimulus (e.g. Johannes et al. 1995). The lateralization of the N1 can reflect a relative spatial coding in the cases where several visual lateralized stimuli appear (Wascher et al. 2009). The N1 is sensitive to task difficulty (Mangun and Hillyard 1991) and is strongly modulated by selective spatial attention (Hillyard and Anllo-Vento 1998; Hillyard and Kutas 1983; Johannes et al. 1995; Luck et al. 1990; Störmer et al. 2009; Vogel and Luck 2000).

2.5.3. P3

The P3 component is later in time: 250 - 500 ms (Hillyard and Kutas 1983; Kelly and O'Connell 2013; O'Connell et al. 2012) or even 350 - 750 ms (Johannes et al. 1995). It was considered that the P3 may reflect cognitive processing and decision making (Hillyard and Kutas 1983; Kelly and O'Connell 2013; O'Connell et al. 2012). It was shown that the P3 reflects the activation of established stimulus-response links during the performance of a task (Verleger et al. 2005, 2014a, 2014b). The amplitude of the P3 can be

sensitive to difficulty of a decision (Verleger et al. 2014a), and negatively correlates with RT (Friedman 1984; Ramchurn et al. 2014; Roth et al. 1978; Verleger et al. 2014a). The P3 also can provide information about intraindividual variability of RTs (Saville et al. 2011). Verleger et al. (2005) found that only the latencies of the P3 varied with RT, whereas the amplitudes were similar. Thus, the different variables of the stimuli and stimulation procedures may affect P3 latency and delay the response times (see review of Verleger 1997).

2.5.4. ERPs of visuospatial perception and attention

The neural correlates of visuospatial perception and attention were investigated using CRT tasks with lateralized visual stimuli. Posner cueing paradigms (Posner 1980) can be used to shift spatial attention to one side of the screen by presenting a cue. These cues can be valid (direct attention to the upcoming stimulus) or unvalid (direct attention from the upcoming stimulus). Endogenuous cues are presented in the center of the center of the screen (Frecska et al. 2004; Mangun and Hillyard 1991; Nobre et al. 1997) and direct the attention by pointing to the side of stimulus. Exogenous cues are presented peripherally and appear in the same location as the stimulus (Fu et al. 2010). It was reported that the P1 and N1 components were enhanced by a valid cue in the CRT task, but only the P1 amplitude was affected in the SRT task (Mangun and Hillyard 1991). The P1 amplitude was higher for high relative low attentional load conditions (Fu et al. 2010). Nobre et al. (1997) found that the P1, N1, and P3 amplitudes were higher for valid cues. Although Frecska et al. (2004) carried out only a behavioural experiment; they reported important findings between healthy subjects and schizophrenic patients: the patients had visual spatial attention deficits in the right visual field.

Cues are not the only way to dirsct the spatial attention to one side of the visual field. The instructions to attend either to the left or the right visual field can be used (Heinze et al. 1990; Johannes et al. 1995; Luck et al. 1990).

The P1 was enhanced over posterior scalp sites contralateral to the attended visual field (Heinze et al. 1990; Johannes et al. 1995; Luck et al. 1990). Heinze et al. (1990) reported that the N2 and P3 amplitudes were larger for target stimuli in the attended visual field, and were reduced or absent for targets in the unattended visual field. The N1 component also was larger for attended stimuli (Johannes et al. 1995). Wascher et al. (2009) used bilateral stimuli and lateralized task-irrelevant stimulus. The authors reported that a task-irrelevant accessory stimulus before bilateral task-relevant stimuli evoked stronger contralateral N1. Thus, accessory modulated visual spatial attention.

In ERP study by Ramchurn et al. (2014), no cues or instructions to direct attention to one side of the visual field were used. They found no effects on the P1 and N1 due to the absence of attentional shift but were able to demonstrate the P3 and RT correlations: the P3 amplitude was significantly greater for faster compared to slower behavioural responses.

Despite differences in paradigms, based on the findings of ERP studies visual P1, N1, and P3 components may be informative for different aspects of visuospatial processing.

2.6. Microstates

Microstates are defined as transient states of EEG topographies. It was proposed that microstates represent the basic building blocks of information processing, because they remain stable for some periods and then rapidly change to a different topographic configuration (Brunet et al. 2011). The concept of functional microstates was first described by Lehmann et al. in 1987. Microstates are obtained from EEG data. Each electrode measures a particular activation at a particular location on the scalp at a time point. The surrounding electrodes also measure activity, which can be important. This spatial distribution of the electrodes allows creating a topographic map at each time point. Microstates can be obtained from spontaneous EEG during rest when no task has to be done (resting-state microstates) (e.g. Kikuchi et al.

2011) and from EEG segments containing an event during the execution of a task (e.g. Koenig et al. 2014). In both cases, the steps taken to obtain microstate maps are the same. **Figure 2.4** shows a basic shema how microstates are obtained from EEG data at each time point and assigned to microstate classes. EEG topographic maps are created at each time point (momentary EEG topographies). A number of topographic classes (clusters) of microstates is calculated. Using the clustering procedures, the momentary maps are assigned to these newly created microstate classes that explain variance of the EEG data (Koenig et al. 1999; Michel et al. 2009). This grouping of momentary EEG topographies is based on the spatial similarity of momentary topographies and cluster maps, and each momentary map is assigned to a single microstate clusted. It is important to mention that the polarity of the map is ignored during the assignment of resting-state microstates (Koenig et al. 1999; Pascual-Marqui et al. 1995), but is important during the assignment of task-related microstates (Pascual-Marqui et al. 1995).

Different topographic configurations of the brain's electric field are considered to reflect activity of different neural networks and, thus, suggest different functions (Koenig et al. 1999). Microstates were provided as an alternative view to the ERPs (Pascual-Marqui et al. 1995). In the cases of the microstates during task, new microstate classes have to be obtained from the ERP data for each task, and polarity must also be taken into account. Moreover, these new classes of microstates should not be considered as final recognition of all brain states that reflect the same function (Pascual-Marqui et al. 1995).

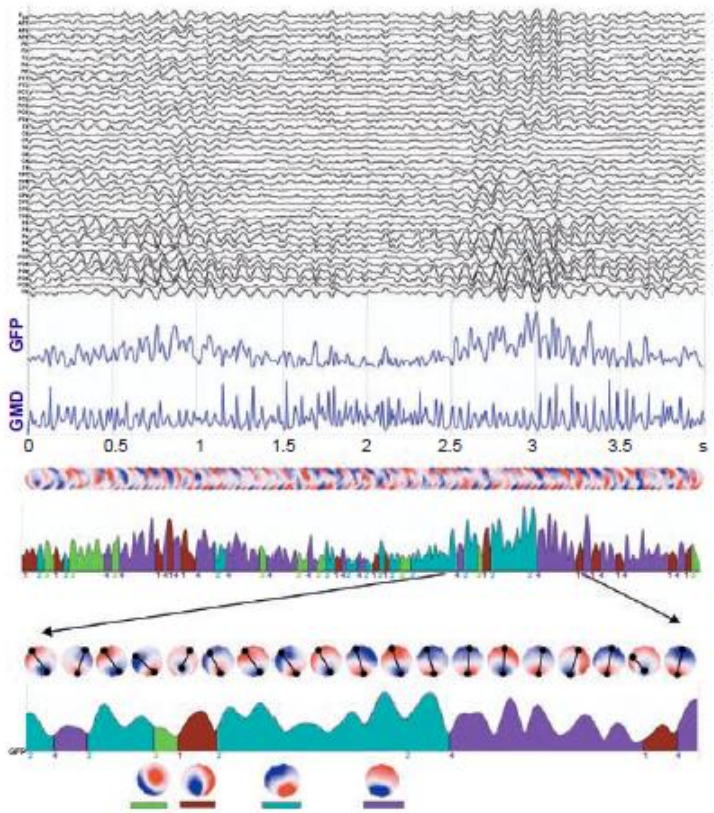

Figure 2.4. Clustering analysis of spontaneous EEG. Similarly, microstate maps are obtained from EEG segments containing events (ERP segments). The EEG data is shown on top. Below the overlapped map series the result of the clustering analysis is shown. In this case, four maps were found to best describe this data. The polarity inverses at each GFP peak but not the topography. Note, that polarity is not important only in the case of resting-state microstates, but it is important if ERP-related microstates are obtained (From Murray et al. 2009)

ERP waveshapes show differences in activation between two recording points. When a multichannel EEG is registered, it can be difficult to choose particular channels to analyse, especially if one does not know what effects to expect. Despite the excellent temporal resolution, the precise measurement of the timing of an ERP component is difficult owing to the fact that ERP components typically overlap with their neighbours (Woodman 2010). In this case, the so-called spatial analysis (microstate analysis) approach has an advantage in that it allows analyzing all scalp fields, and this applied not only to the differences between particular ERPs (Brandeis and Lehmann 1986). The ERPs have a specific scalp distribution which makes them easier to distinguish (Woodman 2010). A microstate class can be assigned to a particular ERP based on latency and topography (Michel et al. 2009). Microstate analysis enables to investigate the differences between distributions of these ERPs (Brandeis and Lehmann

1986). Fallgatter et al. (1997) applied microstates analysis to the EEG data of the Continuous Performance Test and found a robust difference between P300 topographies in the Go and the NoGo conditions. Stevens et al. (1997) observed changes in microstates topography between schizophrenia patients and healthy subjects during mental tasks. Different scalp field topographies are caused by different intracranial sources (Vaughan 1982). Therefore, since microstate maps represent topographies, microstate analysis allows comparing ERPs in terms of topographic maps across conditions and groups (see Murray et al. 2008).

Microstate analysis is a very useful tool for the investigation of networks dynamics (Koenig and Pascual-Marqui 2009). This networks dynamics can be investigated at rest (Koenig et al. 1999; Lehmann et al. 1998, 2005; Strelets et al. 2003; Yuan et al. 2012) and during different tasks (Fallgatter et al. 1997; Kochi et al. 1996; Stevens et al. 1997). The microstate approach is frequently used to investigate the changes of temporal brain dynamics in disease, such as, for instance, schizophrenia (Kochi et al. 1996; Koenig et al. 1999; Lehmann et al. 2005; Stevens et al. 1997; Strelets et al. 2003). Since microstate analysis allows investigating networks, it not only reveals temporal dynamics of processing but also enables to compare EEG data with fMRI data (Musso et al. 2010; Yuan et al. 2012). This is important for visuospatial processing studies where only fMRI findings in networks activation are reported and temporal dynamics have to be revealed. Moreover, because the method is psrticularly sensitive to differences in activation between healthy participants and patients, microstate analysis can be considered a useful tool for screening procedures.

3. Methods

3.1. Participants

In total, 50 subjects participated in two experiments:

22 healthy subjects (14 females, 8 males; mean age 26.7 years, SD = 3.1) participated in the visuospatial and non-spatial judgment study that had visuospatial judgment and color judgment conditions.

28 healthy subjects (17 females, 11 males; mean age 35.6 years, SD = 10.5) participated in the study with lateralized visual stimulation and performed a simple 4-choice reaction time (*CRT*) task.

All participants had normal or corrected to normal vision and were right handed according to a short version of the Edinburgh handedness inventory (Oldfield, 1971), for mean Laterality Quotient (L.Q.) see **Table 3.1**. They had no past history of psychiatric and neurological disorders, as well as head trauma. Subjects were asked to refrain from caffeine and nicotine for at least four hours before their EEG session. They reported to be free of any medication or drugs.

The investigations were approved by the local ethics committee of the canton Bern and conducted in accordance with the Declaration of Helsinki. Informed written consent was obtained from every subject prior to participation.

Table 3.1. Demographic information about the participants of the two experiments.

	Visuospatial and non-spatial judgment	CRT
Age (SD)	35.6 (10.5)	26.7 (2.4)
Female-male ratio	17:11	9:2
L.Q. (SD)	97.0 (7.3)	91.3 (12.1)

3.2. Stimuli and task

3.2.1. Visuospatial and non-spatial judgment task

Examples of stimuli and stimulation scheme are shown in **Figure 3.1a** and **3.1b.** The stimuli were similar to those previously used by de Graaf et al. (2009, 2010) and Sack et al. (2002a, 2007) in fMRI experiments. The visual stimuli consisted of schematic analog clocks with a yellow face and two white or yellow hands presented on a black background. The angle between the clock hands varied in steps of 30°: 30°, 60°, 90°, 120° and 150°.

The "Clock task" consisted of two tasks: visuospatial judgment (angle discrimination – ANGLE) and color judgment (COLOR). The visual stimuli in these two discrimination tasks were physically identical, but the instructions for each task were different. In order to keep the ANGLE and COLOR tasks consistent with the previous studies that used the same task design, particular stimulus categories were assigned to targets and non-targets. In the ANGLE task, targets were clocks with angles of 30° or 60° (small angles) and non-targets were clocks with angles of 90°, 120° or 150° (large angles). In the color discrimination (COLOR) task, clocks with white hands were targets and clocks with yellow hands were non-targets.

A block design with intermixed target and non-target trials was used (see **Figure 3.1b**). In one run, 6 ANGLE and 6 COLOR blocks were presented in alternating order. Prior to each block, a visual instruction cue (ANGLE or COLOR) was projected for 2000 ms. One block contained 10 stimuli. Each stimulus was presented for 300 ms with pseudorandomized interstimulus intervals ranging from 2500 to 3500 ms in steps of 250 ms (equally distributed). During interstimulus intervals, a white fixation cross appeared in the center of the screen. All the stimuli and the fixation cross were equiluminant. For every trial, the response time from the stimulus onset until the button press was measured.

Subjects were comfortably seated on a chair in a darkened, sound-dampened and electrically shielded EEG booth. The stimuli were presented on

an LCD monitor (HP L1950, 19-inch, height – 30 cm, width – 38 cm) placed 40 cm in front of the subject. A chin rest was used to avoid head movements. Before the experimental session, the subjects were asked to fix their gaze at the fixation cross or at the dot in the centre of the clock face (both appeared in the centre of the screen). The participants were instructed to respond as quickly as possible, and to press one of the two keys on the computer mouse with their right index finger for target detection and to press the other key with their right middle finger for non-target stimuli.

The participants performed four runs with a total of 480 trials. Between runs, they rested for a short period. The entire experiment, including the breaks, lasted about 40 minutes in total.

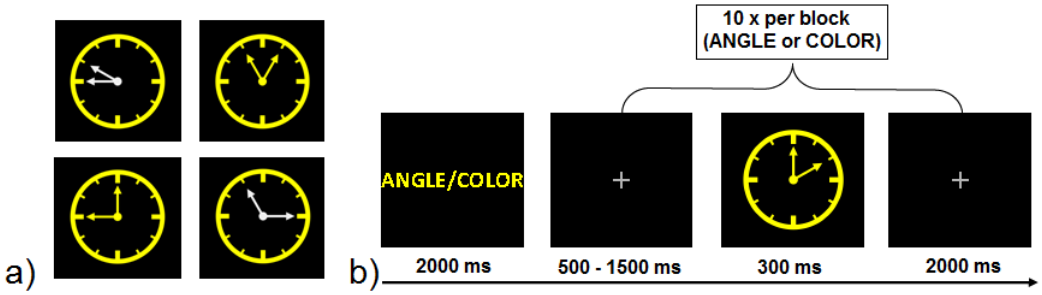

Figure 3.1. a) Example clocks for the visuospatial and color judgment experiment with 30º, 60º, 90º, and 120º between the alternating white and yellow clock hands (as seen from the upper left to the lower right clock). **b)** The experimental paradigm for one block, starting with the block instruction (either COLOR or ANGLE discrimination).

3.2.2. CRT task

The paradigm was adapted from Tuch et al. (2005). The stimuli consisted of four empty squares, presented as the white outlines of squares on the black background. The schematic representation of the stimuli and stimulation procedure are shown in **Figure 3.2**. The squares were horizontally aligned and continuously present on a computer monitor. The white fixation cross was placed between the two medial squares, so that two stimuli were on the left, and two on the right side of the fixation cross. Thus, depending on their location, stimuli were attributed to 4 conditions according to the

stimulation side of the visual field: left lateral (LL), left medial (ML), right medial (MR), or right lateral (RR). In each trial, the target was indicated by filling one of the four squares in with white for a brief period. Thus, the target could occur in one of four locations: LL, ML, MR or RR. In each trial, target appeared for 100 ms. The inter-trial interval was set at 2000 ms (**Figure 3.2**). The task used in our study differed from the one used by Tuch et al. (2005) due to the following modification: The target stimuli were not prevented from reappearing at the same position as in the previous trial, and were presented in a strictly random order.

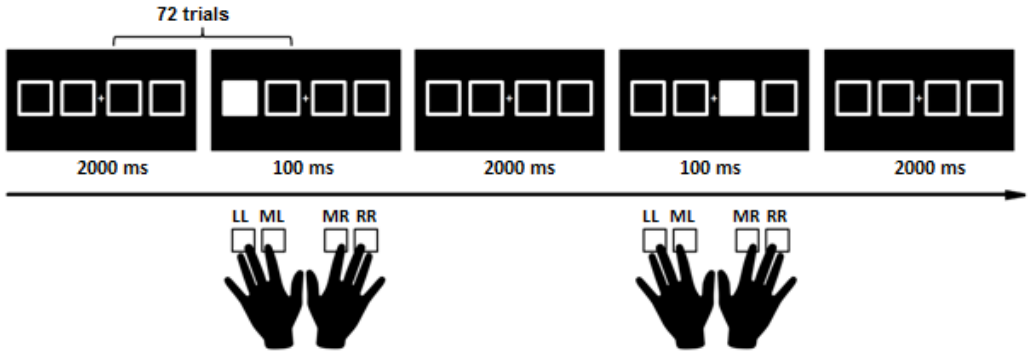

Figure 3.2. Example of stimuli and stimulation procedure for CRT task.

The participants were comfortably seated in a dimmed, acoustically and electrically shielded EEG booth. A computer monitor was placed 120 cm in front of the subject. At this viewing distance, all the four stimuli taken together extended a visual angle of about 6.6 degrees, 1.3 degrees each. Horizontally, the lateral squares extended from 1.82 to 3.12 degrees, and the medial squares extended from about 0.14 to 1.54 degrees. The participants were instructed to fix their gaze at a fixation cross between the two medial squares, to respond to targets as quickly as possible, and to not correct any errors.

During the experiment, the participants rested the index and middle fingers of both their hands on the appropriate keys of a four-key response board (ERTS (Experimental Run-Time System) York, United Kingdom, keyboard with mechanical keys). The responses were given by pressing the corresponding key, whose position was similar to the position of the stimulus.

The corresponding keys were assigned to a finger accordingly: LL stimulus corresponding key – left middle finger, ML stimulus corresponding key – left index finger, MR stimulus corresponding key – right index finger, RR stimulus corresponding key – right middle finger.

The task was repeated in four blocks of 72 trials for a total of 288 trials. Between blocks, participants rested for a short period. The experiment, including the breaks, lasted about 11 minutes in total.

3.3. Acquisition of EEG Data

For the EEG recording, equipment from EasyCap, Falk Minow (Herrsching, Germany) was used. The EEG was recorded using Ag/AgCl ring electrodes mounted in an elastic cap and arranged according to the extended International 10/20 system. Two additional electrooculography (EOG) channels were placed below the left and the right eye to register horizontal and vertical eye-movements. A Neurofax EEG-1100G system amplifier (Nihon Kohden, Tokyo, Japan) was connected to the cap and the EEG was referenced online with the reference electrode. EEG was digitized and stored using a BrainScope EEG system (M&I, Prague).

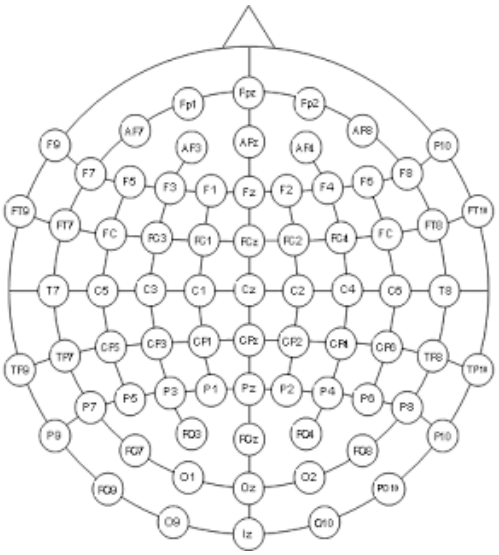

Figure 3.3. EasyCap electrode placement scheme. Note that electrodes O9 and O10 were not used in the visuospatial and non-spatial judgment experiment.

In the visuospatial and non-spatial judgment experiment, 72 electrodes were used (see **Figure 3.3** for a scheme of EasyCap electrode placement, electrodes O9 and O10 were not used) and the reference electrodes were placed at C3 and C4. The impedance was kept below 20 kΩ for all electrodes. The recording filters were set between 0.016 Hz and 120 Hz bandpass and the EEG was digitized with a sampling rate of 500 Hz.

In *CRT* experiment, 74 electrodes were used (see **Figure 3.3** for a scheme of EasyCap electrode placement, all electrodes were used), the reference electrode was Cz. The impedance was kept below 15 kΩ for all electrodes. During the recording, the EEG was amplified and filtered with a 0.3-70 Hz band pass, sampling rate was 250 Hz.

3.4. Analysis of Behavioural Data

A summary of the two experiments is shown in **Table 3.2**. Conditions and factors for the behavioural analysis of two experiments are shown in **Table 3.3**. The mean RT of correctly answered trials and accuracy were calculated separately for each condition and subject.

Predictive Analysis SoftWare (PASW Statistics, Version 22.0.0, Polar Engineering and Consulting) was used to analyze the behavioural data, in particular, to perform the analysis of variance (ANOVA) and t-tests. For ANOVAs, the variables of interest were the reaction time (RT) of correctly answered trials and the accuracy of responses.

In the visuospatial and non-spatial judgment experiment, a two by two factorial repeated-measures analysis of variance (ANOVA) was used to assess main and interaction effects regarding RT and accuracy. The two factors for the analysis were “Task” (angle versus color) and “Stimulus” (target versus non-target).

A five by two factorial repeated-measures analysis of variance (ANOVA) was used to assess main and interaction effects regarding RT of correctly answered trials and accuracy in the Angle task with the factors

"Angle" (angle size) and "Hand" (clock hands color). This ANOVA was followed up by a paired sample t-test analyses. The paired sample t-test was applied to analyse the differences between RTs of correctly answered trials for different angle stimuli (not separated for clock hands color).

Table 3.2. Summary of the two experiments.

	Visuospatial and non-spatial judgment task	CRT task
Task	Visuospatial judgment Color (non-spatial) judgment	Location detection
Stimuli	Clocks	Squares
Stimulus presentation	Central	Lateralized – horizontally aligned
Angular disparities	30°, 60°, 90°, 120°, 150°	-
Modulations	Hands color: white, yellow	-
Difficulty	ANGLE COLOR	-
Target location	Central	LL – left lateral ML – left medial MR – right lateral RR – right medial
Number of stimulus categories	10 (5 angles x 2 hand colors)	4
Target	Angle task: 30°, 60° Color task: White	Location with filled-in square
Non-target	Angle task: 90°, 120°, 150° Color task: Yellow	Empty squares (ignore)
Finger assignment for target	Right index finger	LL stim. – left middle finger ML stim. – left index finger MR stim. – right index finger RR stim. – right middle finger
Finger assignment for non-target	Right middle finger	
Names of conditions	Angle target Angle non-target Color target Color non-target	LL ML MR RR
Number of stimuli per block	10	72
Number of blocks per run	6 ANGLE blocks 6 COLOR blocks	4
Number of runs	4	1
Trials in total	480	288
Duration in total	40 min.	11 min.

In the *CRT experiment*, the answers were treated as outliers and were excluded from further analysis if the participants pressed a response key earlier than 150 ms after the stimulus onset or later than 1000 ms after the stimulus onset. Error rates were calculated separately for errors made by pressing a

wrong key on the stimulated side ("same-side errors"), on the other side ("other-side errors"), and pressing no key in time (omissions). Moreover, omissions were calculated separately for left and right side stimulations. The calculations of the error rates and omissions were similar to the accuracy calculations: the number of wrong responses or no responses was divided from the total number of responses in a particular condition (or conditions). The obtained values range from 0 to 1 (0 to 100 %). The amount of different incorrect responses and missed responses was low. For incorrect answers, the error rate on the same side was 0.015 (SD = 0.016); the error rate on the other side was 0.004 (SD = 0.006); the omission rate was 0.003 (SD = 0.004); omission rates between hemispheres did not vary (0.003 (SD = 0.006) – for left side stimulation; 0.003 (SD = 0.005) – for right side stimulation).

Table 3.3. Conditions and factors for behavioural analysis in two experiments.

	Visuospatial and non-spatial judgment task	CRT task
Variables of interest	Reaction time Accuracy	Reaction time Accuracy
Conditions	Angle target Angle non-target Color target Color non-target	LL ML MR RR
ANOVA 2x2 factors	"Task" (Angle, Color) "Stimulus" (target, non-target)	"Hemisphere" (Left, Right) "Laterality" (Lateral, Medial)
ANOVA 5x2 factors	"Angle" (angle size) "Hand" (hand color)	-

A two-by-two factorial repeated-measures analysis of variance (ANOVA) was used to assess main effects and interaction regarding RT and accuracy. The two factors for the analysis were "Hemisphere" (left versus right) and "Laterality" (medial versus lateral).

3.5. Analysis of ERP Data

The tool used for the preprocessing and basic analysis of the EEG data was Brain Vision Analyzer (Version 2.04, Brain Products, Munich). A chart-flow of EEG processing steps for the two tasks is shown in **Figure 3.4**. First,

the EEG was corrected for vertical and horizontal eye movement artifacts by removing those components identified by an independent component analysis (ICA).

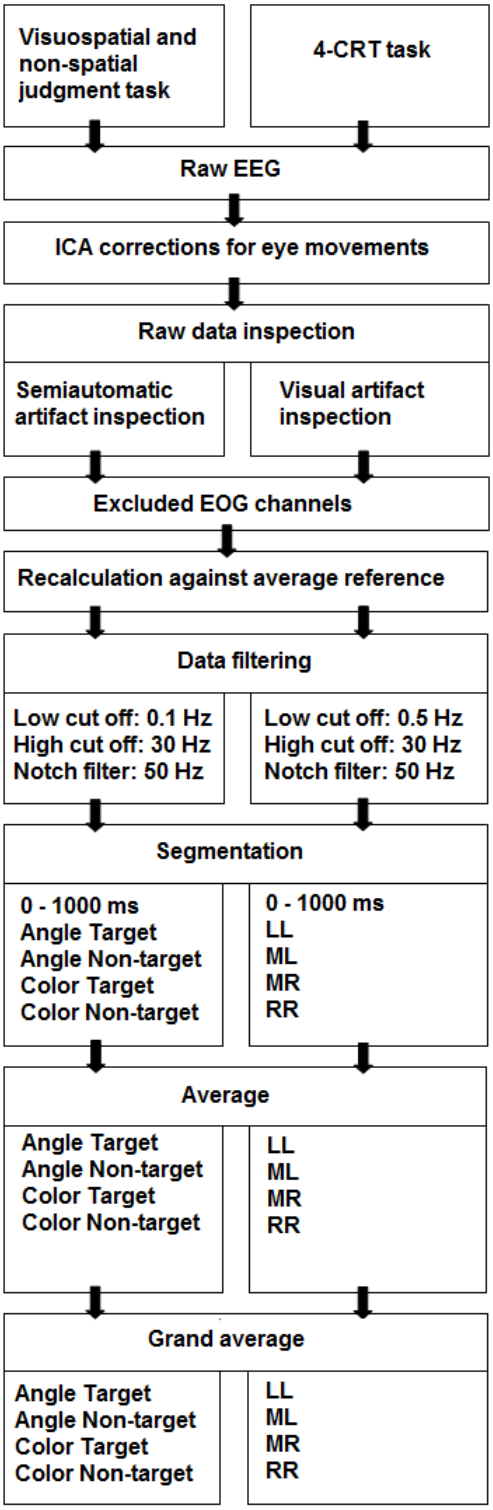

Figure 3.4. The chart-flow of the EEG processing steps for the two tasks. CRT – Choice reaction time, ICA – Independent Component Analysis, LL – left lateral, ML – left medial, MR – right medial, RR – right lateral.

Afterwards, the EEG was inspected and epochs with further artifacts, such as movement or muscle activity, were rejected (see **Figure 3.4**). In raw data inspection step, the channels containing a high amount of artifacts were replaced by a linear interpolation between their neighboring electrodes, which was done for a total of 27 traces out of the 1584 traces (72 times 22) in the visuospatial and non-spatial judgment experiment data. In the *CRT* experiment, no channels containing a high amount of artifacts were recorded, thus the linear interpolation was not used. EOG channels were excluded, the EEG recordings were recalculated against the average reference and filtered (**Figure 3.4**).

To define the optimal end of the time window for the analyses of EEG epochs, the distribution of reaction times for each subject was inspected and the end of segmentation interval was chosen regarding reaction times. For all analyses, the EEGs were segmented for each condition separately. No baseline correction was applied.

Finally, the averages of the epochs representing correctly answered trials were calculated separately for each subject and each condition, followed by the generation of grand mean ERPs across all subjects of each averaged condition (**Figure 3.4**).

3.5.1. Topographic Consistency Test

In order to check a segmented analysis window for the presence of consistant signal across subjects and to determine a useful analysis window with topographic consistencies within it, the Topographic Consistency Test (TCT) (Koenig and Melie-García 2010) was applied. The TCT was performed in the open-source software RAGU (Randomization Graphical User interface; Koenig et al. 2011) based on Matlab (Version 7.6.0.324, R2008a, The MathWorks).

The TCT is a method that allows limiting the data analysis window to periods where a particular event activates the consistent topographies of the

event-related scalp field data across repeated measurements (i.e. single trials, subjects, etc.) related to the experimental conditions (Koenig and Melie-García 2010). Thus, TCT has a significant impact on the further analysis and interpretation of the data, because it reveals periods with constant sets of neuronal sources.

The TCT is based on the nonparametric randomization techniques, and requires a global index of the presence of the scalp field for the computation of the effect size under the null hypothesis. One such index is the Global Field Power (GFP, Lehmann and Skrandies 1980) which shows the strength of a scalp field in the average across observations. Murray et al. (2008) defined the GFP as "a single, reference-independent measure of response strength". Koenig and Melie-García (2010) showed that the GFP can be mathematically equated to the standard deviation across all channels.

The procedure of the TCT is described in detail by Koenig and Melie-García (2009, Chapter 8): The GFP of the grand mean ERPs across subjects is computed with the corresponding mean GFP. Subsequently, the measured potentials are randomly shuffled across the channels, separately for each subject, thus destroying the topographic consistency the across the subjects. Later, the grand mean GFP and the corresponding mean GFP of those randomly shuffled data are computed. The null hypothesis postulates that there is no consistent topography across subjects, thus TCT estimates the probability of the null hypothesis by repeating the randomization procedure a sufficient number of times. The null hypothesis is rejected if the probability of cases where the GFP of the grand mean obtained in the originally observed data is larger than the GFP obtained after randomization.

In the visuospatial and non-spatial judgment experiment, the test for consistent scalp topographies across subjects was applied for each condition (Angle Target, Angle Non-target, Color Target and Color Non-target) separately resulting in four sets of the consistency of the topographies across time. In the *CRT* experiment, the TCT was applied for each condition (LL,

ML, MR and RR) separately resulting in four sets (LL, ML, MR and RR) of the consistency of the topographies across time.

3.5.2. Microstates segmentation and analysis

Microstates segmentation and analysis was performed in RAGU in the following order: The prototype maps of microstates were identified, the optimal number of microstates was found, and then a statistical analysis was performed on microstate parameters (Koenig and Melie-García 2010; Koenig et al. 2014).

To identify microstate prototype maps in the EEG data, the AAHC (atomize and agglomerate hierarchical clustering) algorithm was used: This algorithm segments EEG data into representative topographic maps or microstates for each data point. Subsequently, obtained maps are merged between all conditions and groups, and, after many iterations, the AAHC algorithm creates topographic classes (clusters) of microstates. These cluster maps are based on the mean prototype maps and represent and explain variance in the ERP data (Murray et al. 2008). The momentary (representing a time point) EEG topographies are submitted to a clustering algorithm. This algorithm groups the momentary EEG topographies into a predefined number of classes of topographies. This grouping is based upon the spatial similarity among these topographies, and strives to maximize this spatial similarity among all topographies assigned to the same class. Importantly, each topography is assigned to exactly one class. Once this grouping algorithm has converged, the mean topography of each topographic class is computed, yielding the so-called microstate prototype map of each class.

For the microstate analysis, microstate cluster maps were computed based on the grand average ERPs of each condition. The number of clusters was defined by a cross-validation function reaching a plateau (Koenig et al. 2014).

Table 3.4. Conditions and factors for microstate analysis in the two experiments. AUC – the Area under the curve, LL – left lateral, ML – left medial, MR – right medial, RR – right lateral.

	Visuospatial and non-spatial judgment	CRT
Conditions	Angle target Angle non-target Color target Color non-target	LL ML MR RR
Analysed microstate features	Onset Duration AUC	Onset AUC
Experimentally independent factors	"Task" (Angle, Color) "Stimulus" (target, non-target)	"Hemisphere" (Left, Right) "Laterality" (Lateral, Medial)

The cross-validation procedure requires two sets of microstate classes: the learning set and the test set. The learning set consists of ERPs averaged over a subset of the data. The cross-validation procedure uses a learning set to compute the microstate maps with different numbers of microstate classes. After this, the obtained microstates maps are applied to a test set (remaining data). The variance explained by the microstate maps in this test set is computed as a function of the number of classes, and this is repeated many times with randomly composed learing and test sets. For each number of microstate classes, the results obtained from different test sets are averaged. The number of microstates is optimal where this grand mean correlation reaches the maximum. Based on this optimal number, the final microstate maps are computed using the entire data available (Koenig et al. 2014).

These microstates were later identified in the grand mean ERPs obtained after grand average in Brain Vision Analyzer. These microstates had their dynamics in different conditions and were used to analyze differences in microstate latencies. Statistical significance was obtained by applying a randomization test (Koenig et al. 2014). A randomisation test compares the differences observed in real data with the differences observed in random data sets (the distribution under the null hypothesis). In order to calculate the distribution under the null hypothesis, the grand means of the ERP were calculated for each of the conditions separately. After this, the different features of the same microstates were compared between the conditions. *p values* were obtained using the randomisation procedure: The data of all

subjects and conditions were shuffled 1000 times to yield random data-sets. These new data sets were used to compute new grand mean ERPs. Subsequently, different features of the same microstates were compared between the conditions in these newly created random data sets. The differences between new random ERPs can be explained by the null hypothesis. These differences are then compared to the differences found between the real grand mean ERPs, and *p values* are obtained. *p values* represent the probability that an effect that has been observed by chance is estimated by the percentage of all cases where the differences between the randomized data were greater than differences between the real data sets (Koenig and Melie-García 2010; Koenig et al. 2014).

The onset, duration (except for the *CRT* experiment) and amplitude (the area under the curve, abbreviated as AUC) of microstate classes were measured in each condition separately and compared using microstate analysis techniques. The features of all microstates were compared between conditions using a 2 factorial design, or two experimentally independent factors. For the two experiments, conditions, analysed microstate features and experimentally independent factors of microstate analysis are shown in **Table 3.4**.

4. Results

4.1. Behavioural results

4.1.1. Visuospatial and non-spatial judgment

Mean RT and accuracy were averaged within subjects for each of the four conditions separately. Mean and standard deviations (SD) of RTs and accuracy for each condition are shown in **Table 4.1**. The two-by-two repeated-measures ANOVA regarding RT of correctly answered trials with factors "Task" (angle versus color) and "Stimulus" (target versus non-target) resulted in a significant main effect of the factor Task [F (1, 21) = 100.533, $p < 0.0001$]. Mean RTs were significantly shorter in the Color task as compared to the Angle task (see **Table 4.1**). Neither a significant main effect of the factor "Stimulus" nor an interaction of both factors was obtained. Regarding the accuracy of the responses, the repeated-measures ANOVA revealed a significant main effect of the factor "Task" [F (1, 21) = 7.477, $p < 0.012$]. A tendency of almost significant "Task" by "Stimulus" interaction [F (1, 21) = 4.042, $p < 0.057$] was also observed. Accuracy was significantly higher in the Angle task compared to the Color task, and the tendency of interaction could be explained by a lower accuracy in the Color Target condition compared to other conditions (**Table 4.2**), as confirmed by the paired samples t-test analysis of accuracy in the four conditions. Note that the difference was only about 2.5 – 3 % between the Color Target (93.9 %) and the other conditions (> 96.4 %).

Table 4.1. Accuracy, mean RTs, and standard deviations (SD) for each condition.

	RT (ms)	SD	Accuracy	SD
Angle Target	706.25	120.05	0.966	0.037
Angle Non-Target	714.72	85.35	0.971	0.023
Angle mean	710.49	102.70	0.968	0.030
Color Target	634.80	94.85	0.939	0.065
Color Non-Target	629.50	107.13	0.964	0.037
Color mean	632.15	100.99	0.9511	0.051

Table 4.2. p values and t values (in brackets) (df = 21) of paired sample t-test analysis of accuracy in the four conditions.

	Angle Non-target	**Color Target**	**Color Non-target**
Angle Target	0.591 (0.546)	0.004 (3.208)	0.663 (0.441)
Angle Non-target	-	0.021 (2.499)	0.369 (0.917)
Color Target	-	-	0.034 (2.269)

The mean RTs and accuracies for each clock angle are shown separately in **Figure 4.1**. The five-by-two repeated-measures ANOVA regarding RT of correctly answered trials in the Angle task with the factors "Angle" (angle size) and "Hand" (clock hands color) resulted in a significant main effect of the factor "Angle" [F (4, 84) = 21.990, $p < 0.0001$]. Neither a significant main effect of the factor "Hands" nor an interaction of both factors was obtained.

In the Angle task, as revealed by paired sample t-test analysis of angles (not separated by clock hands color), mean RTs for 60º and 90º angles were significantly longer compared to the 30º, 120º, and 150º angles. Also, the mean RT for the 120º angle was significantly longer compared to the 30º and 150º angles (minimal t-value 2.69 (df = 43), all p-values below 0.01) (see **Table 4.3** for p-values and t-values).

Table 4.3. p values and t values (in brackets) (df = 43) of paired sample t-test analysis of RT in the Angle task for five angles (not separated by clock hands color).

	60º	90º	120º	150º
30º	0.0001 (9.840)	0.0001 (7.582)	0.001 (3.652)	0.163 (1.420)
60º	-	0.300 (1.049)	0.0001 (4.143)	0.0001 (5.205)
90º	-	-	0.0001 (7.441)	0.0001 (11.154)
120º	-	-	-	0.010 (2.690)

The five-by-two repeated-measures ANOVA regarding accuracy in the Color task with the factors "Angle" (angle size) and "Hand" (clock hands color) resulted in a significant main effect of the factor "Angle" [F (4, 84) = 3.944, $p < 0.01$]. Neither a significant main effect of the factor "Hands" nor the interaction of both factors was obtained.

In the Color task, as revealed by the paired sample t-test analysis of angles (not separated by clock hands color), the mean RT for the 120º angle was significantly shorter compared to the 30º, 60º, and 90º angles. Also, the mean RT for the 150º angle was significantly shorter compared to the 90º angle (see **Table 4.4** for p-values and t-values).

Table 4.4. p values and t values (in brackets) (df = 43) of paired sample t-test analysis of RT in the Color task for five angles (not separated by clock hands color).

	60º	90º	120º	150º
30º	0.899 (0.127)	0.760 (0.308)	0.019(2.433)	0.141 (1.499)
60º	-	0.808 (0.245)	0.006 (2.867)	0.072 (1.846)
90º	-	-	0.005 (2.943)	0.043 (2.085)
120º	-	-	-	0.457 (0.751)

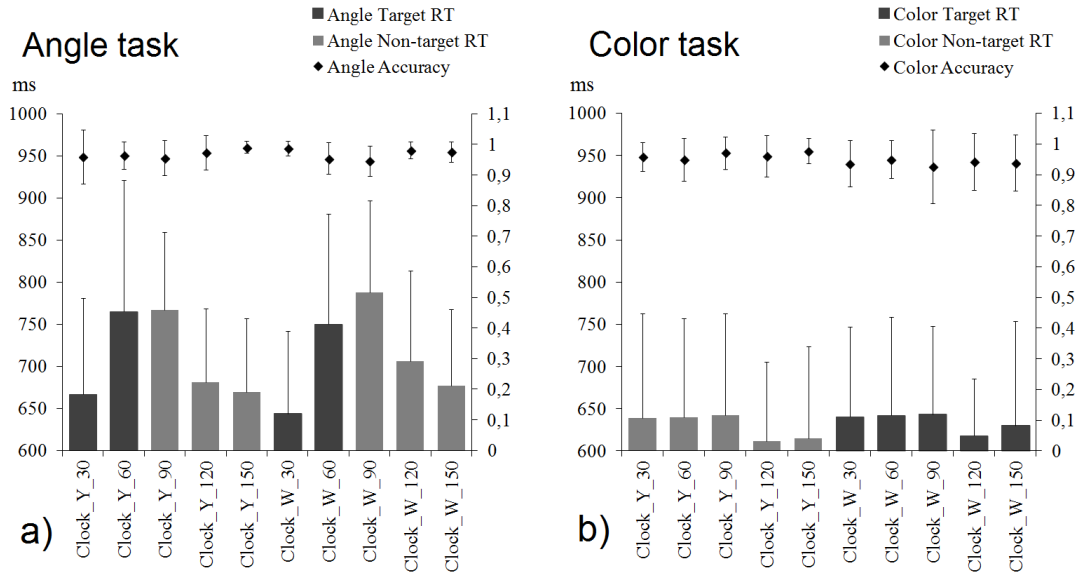

Figure 4.1. Mean RTs and accuracy in **a)** the Angle task, and **b)** the Color task for different stimuli. Y – yellow clock hands, W – white clock hands; the numbers indicate the size of the angle between the clock hands. The different colors of the columns indicate RTs for target and non-target stimuli (see legend). The whiskers indicate standard deviations.

4.1.2. CRT task

Accuracy, mean RTs and standard deviation (SD) for each stimulation condition are shown in **Table 4.5**. All response key presses were observed

within time-limits of correct responses (150 - 1000 ms) and no outliers were found.

Table 4.5. Accuracy, mean RTs, and standard deviations (SD) for each stimulation condition.

	Reaction time (ms)		Accuracy	
	Mean	SD	Mean	SD
LL	449.87	45.88	0.980	0.024
ML	470.37	58.09	0.975	0.027
MR	457.26	56.28	0.970	0.028
RR	435.31	48.67	0.985	0.016

The two-by-two factorial repeated-measures ANOVA on accuracy of responses with factors "Hemisphere" (left versus right) and "Laterality" (medial or lateral) resulted in a significant main effect of the factor "Laterality" [F (1, 27) = 6.132, $p < 0.02$]. Accuracy was significantly higher in the lateral conditions (LL and RR) as compared to the medial conditions (ML and MR). Neither a significant main effect of the factor "Hemisphere" [F (1, 27) = .009, $p < 0.93$] nor the interaction of both factors was obtained [F (1, 27) = 2.600, $p < 0.12$].

Regarding RT of correctly answered trials, the two-by-two factorial repeated-measures ANOVA revealed a significant main effect of the factor "Hemisphere" [F (1, 27) = 7.575, $p < 0.01$]. Mean RT was significantly increased in the left visual field (right hemisphere) conditions (LL and ML) as compared to the right visual field (left hemisphere) conditions (RR and MR). Also, a significant main effect of the factor "Laterality" [F (1, 27) = 12.871, $p < 0.001$] was observed. This main effect was accounted for by the significantly longer RTs in the medial conditions (ML and MR) as compared to the lateral conditions (LL and RR). No significant interaction was observed [F (1, 27) = 0.042, $p < 0.839$].

4.2. ERP results

4.2.1. Visuospatial and non-spatial judgment

The TCT revealed that topographies were consistent across the subjects in the entire analysis window between 0 and 1000 ms (except from 900 ms to 1000 ms in the Color Target condition). The cross-validation of the optimal number of microstates reached a plateau after 10 clusters. The remaining analysis was thus based on 10 microstate classes (MS 1-10). Their respective topographies and times of presence are shown in **Figure 4.2b**. For comparison, waveshapes of the obtained grand average ERPs in four conditions (Angle Target, Angle Non-target, Color Target, and Color Non-target) are shown in **Figure 4.2a**.

The onsets of MS classes 1-3 were similar between the four conditions, as was revealed by the timing of these microstates.

The first differences between the the Angle and Color tasks became apparent with the onset of MS 2 and persisted till the end of the analysis window (MS 10). MS classes 2-10 differed between the Angle and Color tasks in their onset, duration or amount of activation (AUC). Also, the differences between target and non-target stimuli appeared in the time window of MS 5-10, and as **Figure 4.2b** suggests, were most pronounced in the Angle task.

To be more precise, based on latencies and topographies, the obtained microstate classes were assigned to the particular steps of information processing and ERPs (see **Figure 4.2a** and **4.2b**): The first MS class (MS 1) represents a baseline state in which visual cortical activity has not yet been initiated, as well as a transition state. The next three MS classes (MS 2, MS 3, MS 4) represent early visual sensory processing. MS 2 corresponded by latency and topography to the P1 component. MS 3 and MS 4 corresponded by latency and topography to the N1. MS classes 5-8 could be attributed by topography to the P3, and their latency was prolonged (see MS 8). MS 10 was observed after the response. Thus, the statistical analysis was based on MS classes 2-9.

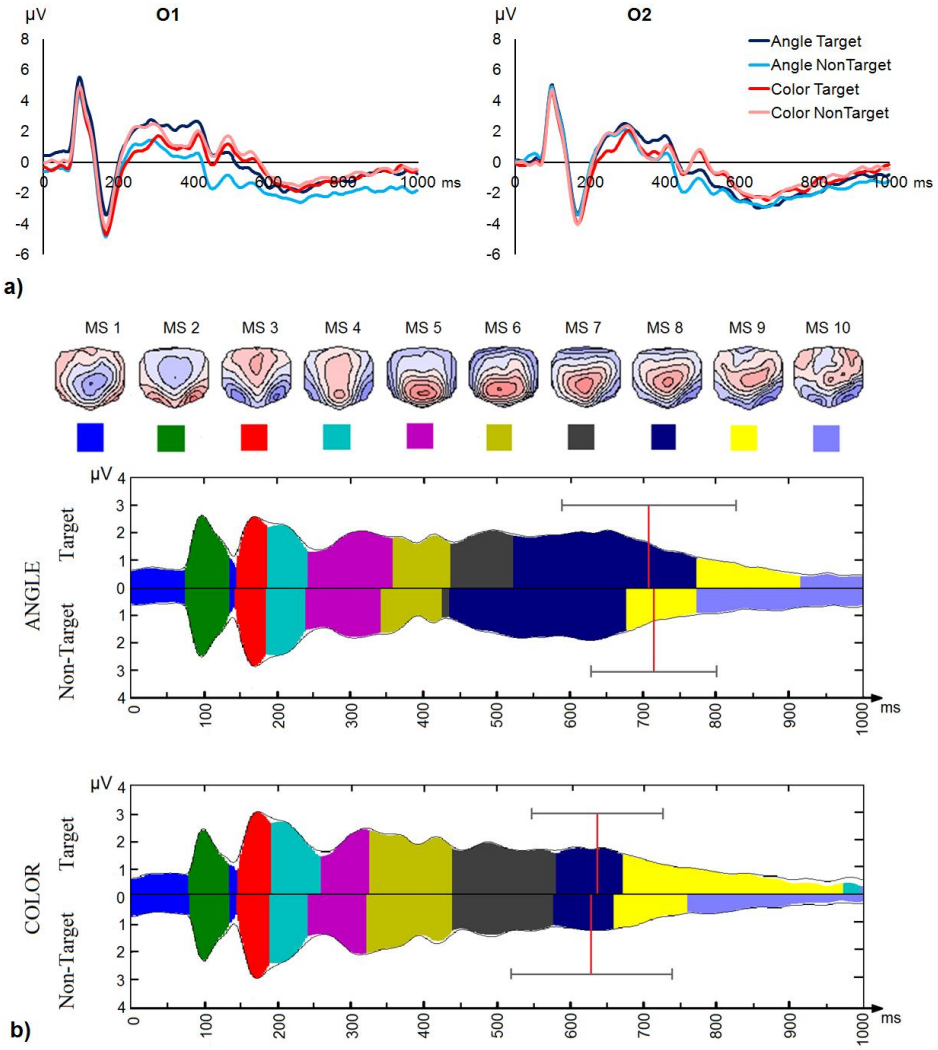

Figure 4.2. a) Waveshapes of the obtained grand average ERPs. Only the waveshapes of electrodes O1 and O2 are presented. The waveshapes show the ERPs of the Angle Target, Angle Non-target, Color Target, and Color Non-target conditions. **b)** MS analysis results. The displays of the target and non-target in the Color task have been flipped vertically and place directly below the corresponding target and non-target displays in the Angle task to facilitate the comparison of the effects. Different colors are attributed to different MS classes. Color indicates the assignment of time to the specific MS class. The height of the colored area indicates the variance explained by the microstate model, while the black curved line enclosing the colored areas represents the GFP. The red vertical lines indicate the mean RT in each condition. The grey horizontal error bars crossing the red vertical lines indicate standard deviation from the mean RT (N = 22). Topographies are shown from above, nose up.

The values of onset, duration, and AUC for MS classes 2-9 are reported in **Table 4.6**. The onset, duration, and AUC of MS 4, MS 5, MS 6, MS 7, MS 8 and MS 9 were chosen for statistical analysis. GFP was not reported, since AUC and duration account for GFP. Statistically significant differences between MS classes were observed from ~ 80 ms to 970 ms. The main findings regarding the onset, duration, and AUC are reported below. For more details,

see the *p values* of the overall analysis and post-hoc analysis presented in **Table 4.7**.

Table 4.6. Onset, duration, and AUC values of MS classes 2-9 (analysis window 0 – 1000 ms).

MS class	Condition			
MS 2	Angle Target	Angle Non-target	Color Target	Color Non-target
Onset (ms)	76	76	78	80
Duration (ms)	60	60	54	54
AUC (ms*µV)	112.2	105.4	91.8	94.3
MS 3	Angle Target	Angle Non-target	Color Target	Color Non-target
Onset (ms)	148	146	146	144
Duration (ms)	42	42	46	46
AUC (ms*µV)	90.3	96.1	113.8	110.2
MS 4	Angle Target	Angle Non-target	Color Target	Color Non-target
Onset (ms)	190	188	192	190
Duration (ms)	54	52	92	52
AUC (ms*µV)	108.8	115.6	155.5	113.9
MS 5	Angle Target	Angle Non-target	Color Target	Color Non-target
Onset (ms)	244	240	260	242
Duration (ms)	116	104	66	80
AUC (ms*µV)	201.7	167.9	127.7	138.0
MS 6	Angle Target	Angle Non-target	Color Target	Color Non-target
Onset (ms)	360	344	326	322
Duration (ms)	80	84	112	116
AUC (ms*µV)	139.2	108.1	226.3	200.8
MS 7	Angle Target	Angle Non-target	Color Target	Color Non-target
Onset (ms)	440	428	438	438
Duration (ms)	84	10	142	138
AUC (ms*µV)	158.6	10.6	232.3	178.7
MS 8	Angle Target	Angle Non-target	Color Target	Color Non-target
Onset (ms)	524	438	580	576
Duration (ms)	250	240	92	84
AUC (ms*µV)	434.7	401.9	146.3	102.4
MS 9	Angle Target	Angle Non-target	Color Target	Color Non-target
Onset (ms)	774	678	672	660
Duration (ms)	142	96	300	100
AUC (ms*µV)	105.6	112.7	222.7	91.5

Table 4.7. p values of the overall and post-hoc statistical analysis of the onset, duration, and AUC of MS classes 2-9 (analysis window 0 – 1000 ms). Significant p values are indicated in bold. Differences between measured values (>) are shown for significant p values and for almost significant tendencies.

MS class	Features	Overall analysis			Post-hoc analysis	
		Task	Stimulus	Interaction	Angle	Color
MS 2	Onset	0.59	0.6	0.97	1	0.48
	Duration	**0.03 (A > C)**	0.69	0.15	1	1
	AUC	**0.004 (A > C)**	0.56	0.14	0.66	0.69
MS 3	Onset	1	1	0.28	0.66	0.57
	Duration	0.57	0.59	0.09	1	1
	AUC	**0.0001 (C > A)**	0.98	**0.035**	0.55	0.64
MS 4	Onset	0.58	0.6	0.22	0.82	0.63
	Duration	0.41	0.053 (T > NT)	**0.02**	0.54	0.19
	AUC	0.27	0.36	**0.029**	0.78	**0.03 (T > NT)**
MS 5	Onset	0.18	**0.007 (T > NT)**	**0.0001**	0.54	**0.007 (T > NT)**
	Duration	**0.0001 (A > C)**	1	**0.004**	0.26	0.27
	AUC	**0.008 (A > C)**	0.54	0.24	0.22	0.79
MS 6	Onset	**0.0001 (A > C)**	0.32	0.15	0.17	0.82
	Duration	**0.0001 (C > A)**	0.73	**0.021**	0.8	0.76
	AUC	**0.0001 (C > A)**	0.17	**0.0001**	0.145	0.17
MS 7	Onset	0.217	**0.019 (T > NT)**	**0.002**	**0.008 (T > NT)**	1
	Duration	**0.0001 (C > A)**	0.28	**0.0001**	**0.006 (T > NT)**	0.7
	AUC	**0.017 (C > A)**	**0.03 (T > NT)**	**0.0001**	**0.0001 (T > NT)**	**0.006 (T > NT)**
MS 8	Onset	**0.0001 (C > A)**	0.2	**0.002**	**0.0001 (T > NT)**	0.7
	Duration	**0.0001 (A > C)**	0.87	**0.014**	0.87	0.46
	AUC	**0.0001 (A > C)**	0.62	**0.02**	0.79	**0.05 (T > NT)**
MS 9	Onset	**0.015 (A > C)**	**0.012 (T > NT)**	0.47	0.008	0.19
	Duration	0.75	**0.043 (T > NT)**	**0.014**	0.23	**0.03 (T > NT)**
	AUC	0.95	0.15	0.08	0.87	**0.047 (T > NT)**

The main effect of "Stimulus" was observed for the onsets of MS 5 ($p = 0.007$), MS 7 ($p = 0.02$), and MS 9 ($p = 0.01$) with an earlier onset for non-target as compared to target conditions. In MS 7, the activation was significantly stronger for target compared to non-target ($p = 0.003$). Duration

of MS 9 was significantly longer for target than for non-target ($p = 0.04$) (see **Table 4.6** and **Table 4.7**).

In the analysis of the "Task" main effect, MSs 2, 5 and 8 were "enhanced" during the Angle task and MSs 3, 6 and 7 during the Color task. In particular, main effects of "Task" were observed in MS 5-8 for duration and AUC, and in MS 6, MS 8, and MS 9 for the onset. MS 5 had a significantly longer duration and higher activation in the Angle task. MS 6 had a significantly earlier onset for Color compared to the Angle task. MS 6 and MS 7, taken together, had a significantly longer duration and higher amplitude in the Color task. MS 8 showed earlier onset, longer duration, and higher activation in the Angle task. MS 9 had a significantly earlier onset for Color compared to the Angle task (see **Table 4.6** and **Table 4.7**).

Significant interactions were observed in all the six MSs selected for statistical analysis: for onset (MS 5, $p = 0.0001$; MS 7, $p = 0.002$; MS 8, $p = 0.002$), duration (MS 4, $p = 0.02$; MS 5, $p = 0.004$; MS 6, $p = 0.002$ MS 7, $p = 0.0001$; MS 8, $p = 0.01$; MS 9, $p = 0.01$), and AUC (MS 3, $p = 0.0001$; MS 4, $p = 0.03$; MS 6, $p = 0.0001$; MS 7, $p = 0.0001$; MS 8, $p = 0.02$). The MS 3 effects are based on the stronger activation of the Color Target condition. The MS 4 effects are based on the longer duration and stronger activation of the Color Target condition. The MS 5 effects are based on later onset and shorter duration of the Color Target condition. The MS 6 effects are based on the longer duration and stronger activation of the Color Target condition, as well as the lowest activation of the Angle Non-Target condition. MS 7 is characterized by the earlier onset of Angle Non-Target and the later onset of the Angle Target condition, and no differences between Color conditions. Duration was the shortest for the Angle Non-Target condition, and was the longest for the Color Target condition (though the difference compared with the Color Non-Target condition was only slight). A similar effect was observed for AUC. MS 8 is characterized by the earlier onset of the Angle Target and the later onset of the Angle Non-Target condition. Duration was the longest and activation was the strongest for the Angle Target condition and effects

were opposite for the Color Non-Target condition. Finally, MS9 is characterized by a specifically longer duration in the Color Target condition. All the relevant post-hoc comparisons are summarized in **Table 4.7**.

4.2.2. CRT task

The cross-validation of the optimal number of microstates reached a plateau after 7 clusters. TCT revealed that topographies were consistent from 0 to 1000 ms in all four conditions, with the exception of the ML condition, which had a period of inconsistency from 636 to 708 ms. The microstates analysis window was limited to the period from 100-1000 ms after trial onset, in order to exclude from the analysis the periods that preceded the appearance of lateralized components.

The microstate topographies obtained in the grand means and their times of presence are shown in **Figure 4.3b**. MS 1 and 2 showed a complementary pattern: MS 1 was primarily evoked by left side stimulation (ML, LL), and MS 2 by right side stimulation (MR, RR). MS 1 and 2 corresponded by latency and topography (occipital negativity contralateral to the stimulus) to the lateralized N1 shown in **Figure 4.3a**. P3 potential corresponded by latency and topography to MS 5. MS 3 was found to be inconsistent (appeared for brief periods) at the very beginning during left side stimulation, and longer periods were consistently observed for all stimulation conditions after MS 6. MS 4 was short and covered transition periods. MS 6 was observer only after the response. MS 7 was observed at the end of the analysis period (see **Figure 4.3b**).

Early lateralized microstates (112-248 ms). In the early time range, the statistical microstate analysis confirmed the complementary pattern of MS 1 and 2. The analysis window for MS 1 and MS 2 ranged from 112 to 248 ms, which corresponded to the period of contralateralization. The results of the microstate analysis are shown in **Figure 4.4** and **Table 4.8**.

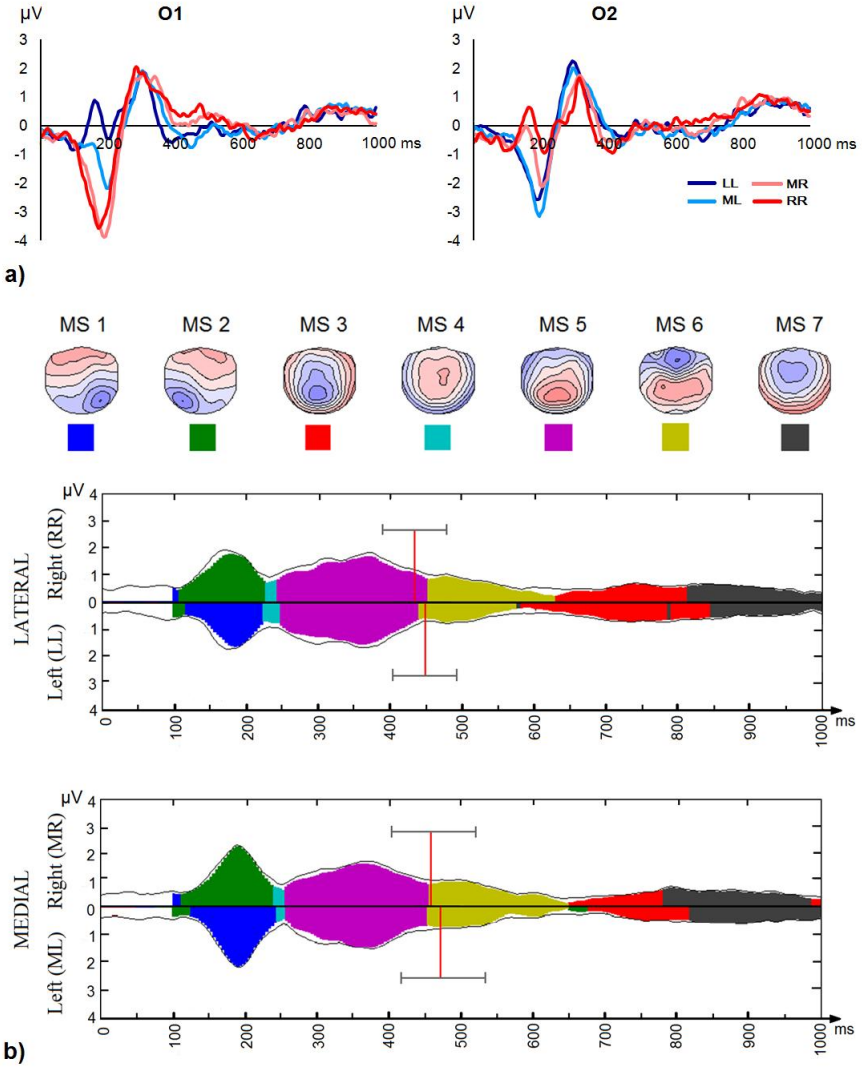

Figure 4.3. a) Waveshapes of the obtained grand average ERPs. Only the waveshapes of electrodes O1 and O2 are presented. The waveshapes show the ERPs of the left lateral (LL), left middle (ML), right middle (MR), and right lateral (RR) conditions. **b)** MS analysis results. The displays of the ML and LL conditions have been flipped vertically and placed directly below the corresponding MR and RR displays to facilitate the comparison of the effects. Colours indicate the assignment of time to the different MS classes, while the height of the areas indicates the explained variance. The thin black curved line following the shape of the coloured areas depicts the GFP; the thick black line indicates the zero baseline. The red vertical lines indicate the mean RT in each condition. The grey horizontal error bars crossing the red vertical lines indicate standard deviation from from the mean RT (N = 28). Topographies are shown from above, nose up.

MS 1 and MS 2. The overall analysis showed a significant main effect for "Hemisphere". Stimulation of the right visual field induced more activity within the left hemisphere (AUC: MS 2, main effect of side: $p = 0.0001$), whereas stimulation of the left visual field evoked more activity in the right hemisphere (AUC: MS 1, main effect of side: $p = 0.0001$). Therefore, these two classes of microstates are associated with early (~110 - 240 ms)

contralateral hemisphere activation. In addition, for MS 2, there was a significant interaction of “Hemisphere” and “Laterality” (AUC p = 0.0001). Post-hoc tests showed that this interaction could be accounted for by larger medial than lateral AUC selectively for the right-side stimulation (p = 0.023).

Later microstates (~ 230 – 1000 ms). Overall analysis of MS 3-7 was performed in the analysis window from 228 to 1000 ms. The beginning of this window was based on the earliest onset of MS 4.

MS 3. The MS 3 analysis revealed a significant main effect of “Hemisphere” for onset (p = 0.047), with an earlier onset for left side stimulation compared to right side stimulation. A significant main effect of “Laterality” was also observed (p = 0.0001), with an earlier onset for the lateral compared to the medial conditions. There was also a significant “Hemisphere” by “Laterality” interaction (AUC: p = 0.03), which could be explained by the earlier onset in left lateral condition compared to other conditions, and the earlier onset in lateral stimulation compared to medial stimulation in the left condition (p = 0.01, difference: 96 ms), but no differences were observed for the right stimulation condition. The overall analysis of the AUC showed a significant main effect of “Laterality” (AUC: p = 0.0001), with higher amplitudes for the lateral as compared to the medial conditions. There was also a significant “Hemisphere” by “Laterality” interaction (AUC: p = 0.0001), which could be explained by a higher amplitude during lateral stimulation compared to medial stimulation in the left condition (p = 0.006, difference: 72.6).

MS 4. Overall analysis of MS 4 showed that the onset was significantly later in the medial compared to the lateral conditions (p = 0.0001). We also observed a significant interaction of “Hemisphere” by “Laterality” (p = 0.0001). This interaction could be explained by a significantly later onset for medial stimulation as compared to lateral stimulation in the left condition (p = 0.01, difference: 20 ms). The analysis of the right condition yielded similar results (p = 0.003, difference: 12 ms).

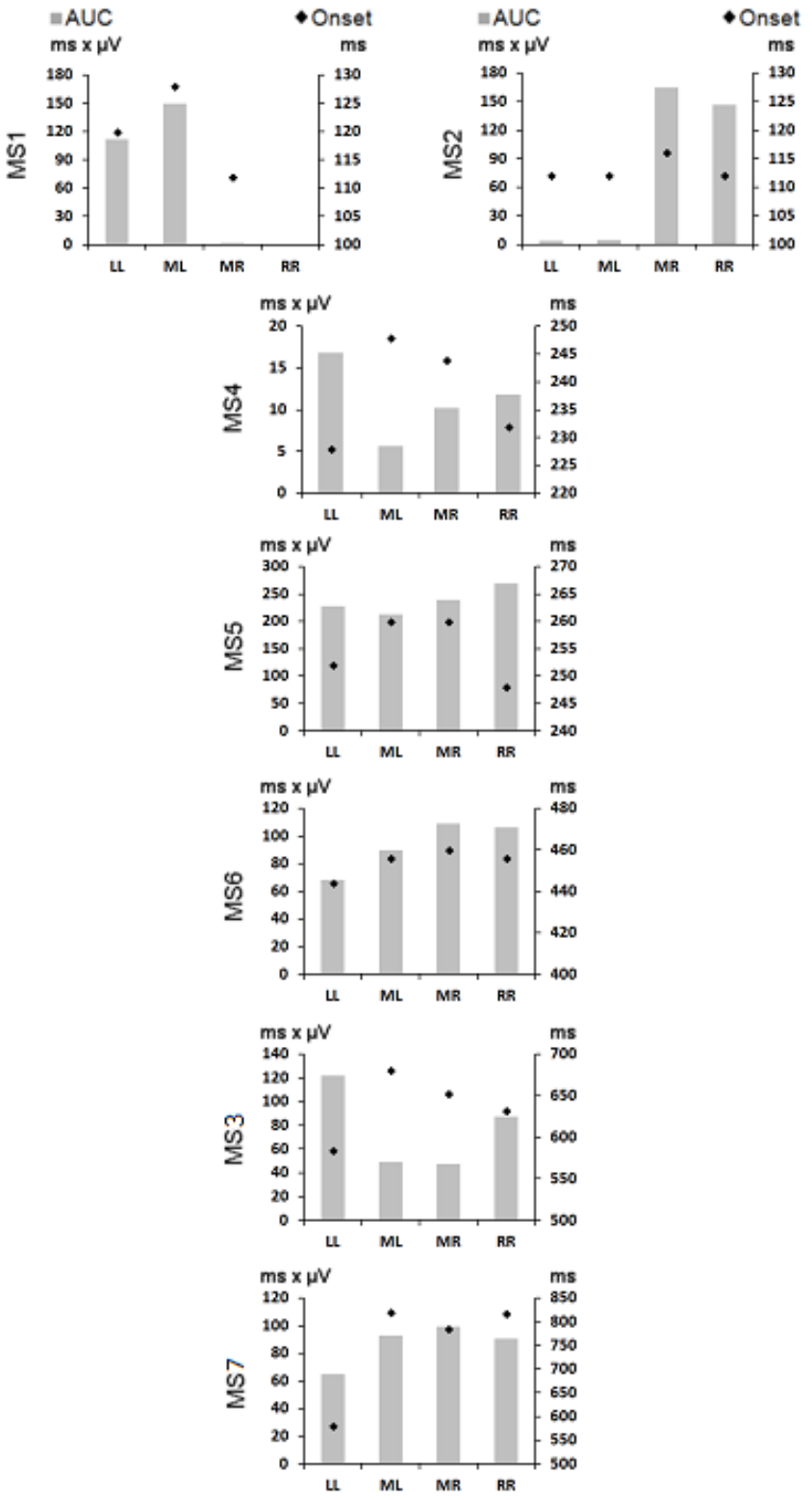

Figure 4.4. The AUC and the onset of MS 1, MS 2, MS 4, MS 5, MS 6, and MS 7. The values of MS 1 and MS 2 are taken from the analysis interval of 112 - 248 ms, while the values of MS 3-7 are taken from the analysis window of 100 - 1000 ms. For MS 1 and MS 2, on the ipsilateral side, the onset of MS 1 is offset of MS 2 and vice versa. The onset of a new microstate is the offset of the previous microstate. Note that the microstates arise in time in the following order: MS1/2, MS 4, MS 5, MS 6, MS 3, and MS7, and this is the order they are presented in. Note that AUC and onset axis values differ for each MS.

Table 4.8. The p values of statistical analysis of microstate features (onsets and AUCs). MS 1 and MS 2 analysis interval was 112 - 248 ms, and MS 4-7 analysis window was 100 - 1000 ms. The left half of the table shows the two main effects and interaction effects of 2 x 2 analyses including all conditions. The right half of the table provides post-hoc results of subsets of conditions where it was justified by the result of the analysis that involved all conditions. A '-' (dash) indicates that a particular contrast could not be computed because a microstate was not observed in one of the conditions included in the contrast.
Med = medial, Lat = lateral, L = left, R = right.

MS class	Statistics ($p < 0.05$)						
MS 1	Overall			Left	Right	Medial	Lateral
	L-R	Med-Lat	L-R*Med-Lat	LL-ML (ML > LL)	RR-MR	ML-MR (ML > MR)	LL-RR (LL > RR)
Onset	-	0.87	-	0.28	-	0.87	-
AUC	*0.0001*	0.83	0.14	*0.0001*	0.47	*0.0001*	*0.0001*
MS 2	Overall			Left	Right	Medial	Lateral
	L-R	Med-Lat	L-R*Med-Lat	LL-ML	RR-MR (MR > RR)	ML-MR (MR > ML)	LL-RR (RR > LL)
Onset	1	1	0.46	1	0.73	0.33	-
AUC	*0.0001*	0.57	*0.0001*	0.72	*0.023*	*0.0001*	*0.0001*
MS 3	Overall			Left	Right	Medial	Lateral
	L-R	Med-Lat	L-R*Med-Lat	LL-ML	RR-MR	ML-MR	LL-RR
Onset	*0.047*	*0.0001*	*0.03*	*0.01*	0.09	0.35	*0.013*
AUC	0.21	*0.0001*	*0.0001*	*0.006*	0.06	0.89	0.056
MS 4	Overall			Left	Right	Medial	Lateral
	L-R	Med-Lat	L-R*Med-Lat	LL-ML	RR-MR	ML-MR	LL-RR
Onset	1	*0.0001*	*0.0001*	*0.01*	*0.003*	0.82	0.66
AUC	0.35	0.18	0.31	*0.02*	0.68	0.33	0.42
MS 5	Overall			Left	Right	Medial	Lateral
	L-R	Med-Lat	L-R*Med-Lat	LL-ML	RR-MR	ML-MR	LL-RR
Onset	1	*0.0001*	*0.02*	0.12	*0.01*	1	0.87
AUC	*0.0001*	*0.04*	0.70	0.35	0.06	*0.022*	*0.02*
MS 6	Overall			Left	Right	Medial	Lateral
	L-R	Med-Lat	L-R*Med-Lat	LL-ML	RR-MR	ML-MR	LL-RR
Onset	0.053	0.88	0.055	0.18	0.91	0.96	0.15
AUC	*0.0001*	0.019	*0.005*	0.065	0.74	0.11	*0.02*
MS 7	Overall			Left	Right	Medial	Lateral
	L-R	Med-Lat	L-R*Med-Lat	LL-ML	RR-MR	ML-MR	LL-RR
Onset	0.22	*0.0001*	*0.0001*	*0.003*	0.41	0.26	0.18
AUC	0.25	0.16	0.07	0.22	0.69	0.74	0.18

MS 5. MS 5 latency and topography corresponded to the P3. The overall analysis showed that the onset was later in the medial compared to the lateral conditions ($p = 0.0001$), and a significant "Hemisphere" by "Laterality" interaction for onset was also observed ($p = 0.02$). This interaction could be

explained by a significantly earlier onset for lateral compared to medial stimulation after right side stimulation ($p = 0.01$, difference 12 ms), while no such difference could be found for the left side. The overall analysis of the AUC showed a significant main effect of "Hemisphere" (AUC: $p = 0.0001$), with higher amplitudes for right compared to left conditions. There was also a main effect of "Laterality", with activation in lateral conditions being stronger than in medial ones ($p = 0.04$).

The mean RT values in each condition were close to the offset of MS 5/onset of MS 6: LL – 449.87 ms, ML – 470.37 ms, MR – 457.26 ms, 435.31 ms (see **Figure 4.3b**).

MS 6. In MS 6, the overall analysis showed a significantly higher brain activation for right side stimulation than for left side stimulation (AUC: $p = 0.0001$) and a significant "Hemisphere" by "Laterality" interaction was also observed ($p = 0.005$). Further analyses accounted for this interaction by a larger AUC in the right lateral compared to the left lateral condition ($p = 0.02$), while no such difference was found in the medial conditions.

MS 7. In MS 7, the overall analysis showed that the onset was later in medial compared to lateral conditions ($p = 0.0001$) (due to the short period of MS 7 covering the transition time between MS 6 and MS 3) and a significant "Hemisphere" by "Laterality" interaction was also observed ($p = 0.0001$). This interaction could be explained by a significantly earlier onset for lateral compared to medial left side stimulation ($p = 0.003$, difference 240 ms), but no such difference could be found for the right side.

5. Discussion

The aim of this study was to investigate the visuospatial temporal dynamics of information processing in visuospatial and non-spatial judgment and in a CRT task with lateralized visual stimuli and to use EEG microstates technique in order to verify these paradigms for EEG studies.

5.1. Networks activation in visuospatial and non-spatial judgment

The same microstates were obtained for visuospatial and color judgment. MS 2 showed topography with stronger positive activity over the right compared to the left occipital electrode site and was attributed to P1 component. N1-related microstate MS 3 showed topography with bilateral negativity over the occipital electrode site that was stronger in the right hemisphere. Later microstates (arising after 400 ms) showed widely distributed parietal and occipital positivity, with the gradients being stronger over the right parietal cortex (MS 7 and 8). This is in line with previous observations, because the same cortical networks were activated during visuospatial judgment and non-spatial judgment tasks but with different strength (de Graaf et al. 2010): the posterior parietal cortex and middle frontal gyrus for the Angle task; the supramarginal gyrus, an anterior region of middle frontal gyrus, and the superior frontal gyrus for the Color task.

Differences in the strength of the BOLD signal could occur due to a difference in the number of activated neurons and/or in the duration of the activation. If the BOLD differences were caused by a larger number of neurons firing at the same time, this would increase the GFP of the microstate and indicate a higher efficiency. If the BOLD differences resulted from a longer activation of the particular brain areas, this would affect the duration of the corresponding microstate, and could indicate more difficulties with the particular information processing step.

It could be summarised that visual information processing undergoes similar steps but only several task specific or task sensitive steps can be affected. The microstates approach is very useful for detecting and analyzing changes in the onset, strength or duration of a particular step. EEG microstate analysis has enabled to establish the differences in temporal dynamics within the same networks during visuospatial processing: In visuospatial and non-spatial judgment task, P1-MS 2 had stronger activation in visuospatial (Angle) judgment compared to non-spatial judgments task, while N1-MS 3 showed the opposite effect. P3-related microstates 5 and 8 were longer and had stronger activation in visuospatial judgment task and MS 8 appeared earlier in Angle judgment task. In contrast, the other P3-related microstate classes – MS 6 and MS 7 – were longer and had stronger activation in the non-spatial color judgment task, and MS 6 appeared earlier in the non-spatial judgment task. RTs were longer in the visuospatial compared to the non-spatial judgment task.

5.2. Reaction time in visuospatial judgment and non-spatial judgment

Behavioural analysis revealed that RTs were shorter in the color compared to the angle judgment; this was confirmed by a significant main effect of the factor "Task" regarding the reaction times of correctly answered trials. Previous studies using the same visuospatial and non-spatial judgment task (Sack et al. 2007; balanced designs in Graaf et al. 2009, 2010) reported similar findings. However, de Graaf et al. (Graaf et al. 2009, 2010) reported smaller differences between the two tasks, which could be accounted for by the balanced design between target and non-target stimuli in the angle (1:1) compared to the color (1:1) conditions. In contrast, Sack et al. (2007) used an unbalanced design: the ratio between target and non-target stimuli was (2:3) in the angle task and (1:1) in the color task.

There is no separate RT data available for each angle size from previous studies (de Graaf et al. 2009, 2010; Sack et al. 2002a, 2007), thus the results from our visuospatial and non-spatial judgment experiment cannot be

compared with the results in existing literature. Only Vannini et al. (2004) reported separate behavioural data for different angles. However, that study a different version of the "Clock task": with different angle sizes and manipulations of the length of clock hands. Despite these differences, the behavioural results obtained during our visuospatial and non-spatial judgment experiment were comparable to the study of Vannini et al. (2004): when the difference between the size of target and non-target angles decreased, RT gradually increased. In more detail, RT increased with angles up to 90º, because the target angles were smaller (30º and 60º), and decreased with larger angles (120º and 150º).

The accuracy of the subjects' performance was high (mean total accuracy = 0.96, SD = 0.041) indicating that the task was not too difficult. Regarding the accuracy of the responses, a significant main effect of the factor "Task" was obtained. The higher accuracy was found for non-target stimuli than for target stimuli, with a bigger difference in the color task.

5.3. ERPs in visuospatial judgment and non-spatial judgment

Previous studies found brain areas and networks involved in visuospatial and non-spatial judgment (de Graaf et al. 2009, 2010; Sack et al. 2002a, 2007).

In visuospatial and non-spatial judgment experiment, the EEG/ERP technique and microstate analysis were applied to establish the temporal dynamics of these networks activation. Microstate analysis allowed comparing cortical activation dynamics between the two tasks: visuospatial judgment and color judgment. The first differences started from the onset of MS 2 (~ 75 ms) corresponding to the P1 component, with the stronger activation in the Angle task. Since the stimuli were identical in both tasks, these differences can be explained by an enhancing spatial attention effect in more difficult task (Fu et al. 2010). Notable differences are observed from ~ 188 ms with the onset of MS 4. Thus, the shift in networks recruitment was found to begin at the late

phase of the N1 (Hillyard and Kutas 1983), although the same networks are generally active during all conditions.

The order of microstates did not differ between the conditions, which may indicate that the processing of incoming information has to undergo the same steps both in non-spatial and spatial tasks. Only the onset, and especially the duration and strength of a specific topography can differ between two judgment tasks. Hence, no unique activation patterns were found. The first four microstate classes (MS 1-4) were similar in their onset across experimental conditions. This similarity suggests the high consistency of the early sensory information processing steps. Early microstate classes (MS 2-4) reflected early visual sensory processing: MS 2 corresponded by latency and topography to the P1, and MS 3-4 corresponded by latency and topography to the N1. These early sensory components (or visual evoked potentials) are known to be evoked by the appearance of a stimulus, and can be modulated by the features of visual stimuli (Butler et al. 2007; Foxe et al. 2001; Oka et al. 2001; Schechter et al. 2005) as well as by selective attention (Gomez Gonzalez et al. 1994; Hillyard and Anllo-Vento 1998; Mangun and Hillyard 1991). It was noticed that P1-MS 2 had longer duration and stronger activation in the Angle task. The stimuli for both tasks were identical, so that activation was modulated by attention only: angle discrimination required more attentional resources, therefore the P1 amplitude was enhanced (Fu et al. 2010).

The main interest of the current study was the cognitive processing of visuospatial judgment, thus the later cognitive components were analyzed. Although the first differences related to visuospatial judgment in the context of the two different tasks occurred at ~ 80 ms post stimulus, the later microstate classes (MS 5-8) showed more differences between the conditions.

The sequence of cognitive components (MS 5-8) was characterized by a relative shift between these microstates for the task conditions. MS 5 and MS 8 activation was more extensive and pronounced for the Angle condition, and MS 6 and 7 activation was more specific for the Color condition. Interestingly, the offset of MS 6 occurs around the same time (~435 ms) in all conditions, so

RT differences cannot be explained by the relative emphasis of task-specific components in the early time window. Differences are more pronounced in the late phase of cortical activity. MS 8 dominates as the late cognitive component of processing during the Angle task and is much more extended in time, presumably producing the increase in RT for the Angle conditions. In the Color task, MS 8 activation is observed at the time window around the button press.

As a summary of these findings, it can be suggested that particular networks represented by MS classes 6 and 7 were more important for color information processing, whereas the networks represented by MS classes 5 and 8 were more important for spatial information processing. In MS 5 and 6, the strongest gradients were observed bilaterally over the parietal cortex, but the gradients over the frontal regions occurred in different places: MS 5 differed from others with widely distributed frontal negativity, while MS 6 had more positivity over the right hemisphere. MS 7 was significantly shortened and MS 8 was significantly prolonged during the visuospatial judgment task.

In MS 7 and 8, the strongest gradients were observed over the right parietal cortex and weaker ones over the frontal regions, but the distribution of positive and negative activation was slightly different between the microstates. These findings could be in line with fMRI data, where an increased activity in parietal and frontal regions was observed during the execution of both tasks, as reported by Sack et al. (2007).

5.4. Reaction time to lateralized visual stimuli

Since microstate results of visuospatial and non-spatial judgment showed stronger activity lateralized to the right hemisphere, it was expected that the *4-CRT* task would reveal more lateralized activation.

The results of the *4-CRT* task showed that RTs were shorter for lateral compared to medial stimuli, and that right hand responses were faster than left hand responses. This task was the same as the one used in DTI study by Tuch

et al. (2005). However, Tuch et al. (2005) reported only mean individual RTs, but found larger negative correlations between RT and white matter properties in the right hemisphere.

Different other SRT and CRT studies report contradictory results regarding RT and response hand.

Annett and Annett (1979) found that the majority of participants reacted faster to stimuli presented to the left visual field and that left hand responses were faster than right hand ones. Moreover, the authors reported that these findings did not correlate with handedness. Faster left hand responses were also observed in a more recent CRT study (Barthelemy and Boulinguez 2001).

Other SRT (Kalyanshetti and Vastrad 2013) and CRT (Steel et al. 2002) studies found that right hand responses were faster. These two groups of researchers used different tasks with centrally presented stimuli and without cues, but the instructions were similar: the participants were instructed to respond to one stimulus with the left hand, and to use the right hand to respond to the other stimulus. Right-handed subjects demonstrated faster right hand responses, and this right hand superiority was observed in SRT tasks with stimulation of different modalities – visual, auditory and cutaneous (Kalyanshetti and Vastrad 2013). The mentioned tasks were different from the one applied in the *CRT* experiment due to the position of the stimuli: in the *4-CRT* task, the stimuli were lateralized. Therefore the behavioural results are not directly comparable. Regarding handedness, all participants were right-handed, thus the dominance of the right hand is in line with the findings of two previous studies (Kalyanshetti and Vastrad 2013; Steel et al. 2002). Nobre et al. (2000) also reported shoerter RTs to stimuli in the right visual field compared to the left visual field; however, there were no differences in RT between response hands.

In contrast, studies that applied Posner cueing paradigms (Posner 1980) reported significantly faster left hand responses: Bestelmeyer and Carey (2004) used lateralized visual stimuli and auditory cues assigned to a particular side of stimulation, and Frecska et al. (2004) applied a complex task with two

lateralized targets and two types of midline cues (stimulus location cue or response hand cue). The faster left hand responses could be accounted for by the effect of the cues, because cueing enhanced the activation of the visuospatial attentional networks predominantly in the right hemisphere. Frecska et al. (2004) interpreted these findings as the right hemisphere dominance in visuospatial processing. However, due to the complexity of their task and the use of cues, results of our *CRT* experiment cannot be directly compared to the findings of these studies.

A simpler task was used by Kolev et al. (2006): they applied a 4-CRT task with 4 centrally presented letter stimuli or corresponding auditory stimuli where each stimulus was assigned to a particular finger. RT for each finger did not differ across both the modalities. Responses given with the left index finger were the slowest. This finding corresponds to the findings in the *CRT* experiment, because the same finger produced the slowest responses (ML condition). The shortest RT was observed for the right middle finger (RR condition), but in the study carried out by Kolev et al. (2006) the shortest RT was found for the right index finger. However, the findings of these two studies cannot be compared directly due to different presentations and characteristics of stimuli – cenltraly presented verbal stimuli in Kolev et al. (2006) versus horizontally aligned and lateralized geometric stimuli in our *CRT* experiment. In both hands, the index fingers responses were slower than middle fingers responses. This is in line with RT findings reported by Annett and Annett (1979). They used lateralized stimuli in SRT and 4-CRT tasks and found that the right index finger was slower than the right middle, left index and left middle fingers, and, similarly, the left middle finger tended to be faster than left index finger. Only one difference exists between the two studies: in the *CRT* experiment the slowest responses were observed for the left index finger but not for the right index finger.

It is possible that the eccentricity of the stimuli was important and affected RT, because lateral stimuli evoked faster responses than medial ones.

5.5. ERPs to lateralized visual stimuli

5.5.1. Early lateralized ERPs (~ 100 – 250 ms)

As expected, the *CRT* experiment revealed early lateralized brain activity: MS 1 represented the N1 potential lateralized to the right hemisphere and MS 2 represented the N1 potential lateralized to the left hemisphere. However, the early ERP component P1 was not found. It usually appears 80 - 130 ms after stimulus onset (Hillyard and Kutas 1983; Johannes et al. 1995) and shows a higher amplitude contralateral to the stimulation side (Mangun and Hillyard 1991). Cueing modulates the amplitude of the P1 due to its sensitivity to attention (Heinze et al. 1990; Hillyard and Anllo-Vento 1998; Johannes et al. 1995; Luck et al. 1990), however, the P1 is evoked in both cued and uncued conditions (Mangun and Hillyard 1991; Störmer et al. 2009). Similarly to Ramchurn et al. (2014), cues were not used in the *CRT* experiment, but the authors did observe the P1. It is known that the P1 is sensitive to stimulus characteristics (Johannes et al. 1995; Michel et al. 1992): Michel et al. (1992) observed the P1 for high contrast stimuli, but low contrast stimuli did not evoke this component. In our CRT task, we used high contrast stimuli; nevertheless, the P1 component was not found.

In previous studies, lateralized stimuli were presented around a fixation point (Luck et al. 1990) or aligned horizontally, but above the horizontal meridian (Fu et al. 2010; Heinze et al. 1990). In the experiment of Ramchurn et al. (2014), stimuli were aligned similarly to our *CRT* task but, in contrast to our *CRT* experiment, the stimulus interval was brief. Although in the *CRT* experiment the target appeared for 100 ms, the square stimuli were presented continuously, and that may have affected the P1. Thus, the absence of the P1 component could possibly be explained by the particular setup of stimuli, that is, by a horizontal orientation and continuous presentation, where only a relatively small part of the screen changed during the stimulation.

Microstates representing the N1 (MS 1 and MS 2) were distributed over the occipital and parietal electrode sites, with negative peaks over the

hemisphere contralateral to the stimulation side. Other studies also showed the N1 component contralateral to the stimulation side (Fu et al. 2010; Störmer et al. 2009; Whitford et al. 2011) and this is in line with current findings. The temporal range of N1-related microstates was similar to the usual latency of the N1 – 140 - 200 ms after the stimulus onset (Hillyard and Kutas 1983; Johannes et al. 1995). Vogel and Luck (2000) compared the N1 between different CRT and SRT tasks, and confirmed that the visual N1 component is an index of discrimination and attention processes, including spatial attention.

The AUC of the N1 was larger over the left hemisphere (MS 2 > MS 1). This is confirmed by a post-hoc analysis of the GFP that yielded a period of a consistent main effect of GFP for the factor side in the time window 136 ms to 164 ms. The result is in line with the literature that reported stronger N1 activation over the left hemisphere (Nobre et al. 2000). However, Nobre et al. (2000) used predictive cues to shift spatial attention to one side or the other, and showed that a higher N1 amplitude could be affected both by lateralized stimulation and attention.

Interestingly, a significantly stronger N1 activation was found for medial (ML, MR) compared to lateral stimulation (LL, RR). These findings may be explained by the fact that medial stimuli stimulate a more binocular visual field due to faster interhemispheric transfer for medial stimuli (Iacoboni et al. 1994).

5.5.2. Later ERP component (~ 250 – 460 ms)

The P3 component, corresponding by latency and topography to MS 5, had a widely positivity distributed over the bilateral occipital, parietal and central electrode sites, with a maximum at Pz. This P3 was observed in all conditions. This appearance in all conditions is fully in line with the P3 literature. It was proposed that the P3 is evoked in every task where a fast decision about the stimulus is required (see Verleger 1997), or “a model of the environment must be revised” (Donchin and Coles 1988), or the context has to

be updated (Donchin 1981; Donchin and Coles 1988). It was also suggested that the P3 is observed "when stimulus detection engages memory operations" (see Polich 2007).

In the *CRT* experiment, the design of our study did not engage memory operations, because participants responded to the location of each new stimulus and were not instructed to remember the location of the previous stimuli. Thus, such a task would be a decision task about the action related to the stimulus (Verleger 2008).

Significantly higher brain activation (P3 amplitude AUC) was observed for the right hemifield/left hemisphere stimulation compared to the left hemifield/right hemisphere stimulation. In addition, we observed the faster right hand responses. This increase in P3 amplitude correlates with faster RT, and such correlation between higher P3 amplitude and faster RTs was reported in several previous studies (Friedman 1984; Ramchurn et al. 2014; Roth et al. 1978; Saville et al. 2011). The strongest activation was in the same condition where the shortest RT was observed – that is, the RR condition. As expected, the opposite P3 activation pattern was observed in the ML condition with the slowest RT: A significant main effect of lateralization ($p = 0.026$) was found. The AUC was higher in the lateral compared to the medial conditions. However, no significant interaction of side and lateralization was observed.

5.5.3. Other ERP components

MS 6 occurred only after the response, and had parietal positivity and frontal negativity that formed strong gradients near the motor cortex. Frontal negativity had a peak over the frontocentral electrodes. Frontocentral negativity occurred 0 - 150 ms after the response and was reported to reflect correct response evaluation in humans (Suchan et al. 2003; Suchan et at. 2007). Thus, the conclusion that MS 6 may correspond to evaluative processes is fully in line with the existing literature. Similarly to MS 5-P3, MS 6 showed a lateralization effect, with a significantly higher brain activation for the right

side compared to the left side stimulation (AUC: $p = 0.003$). This finding may reflect right hand dominance.

These findings complement the knowledge about the visuospatial processing of lateralized stimuli and network involvement.

5.6. Relation between ERPs, RT and stages of information processing

Sternberg (1969) proposed the Additive Factor Model to study processing stages with regard to RT. The Additive Factor Model decomposes stimulus processing into a set of stages, from the stimulus onset to the response. The suggested stages of the information processing were stimulus encoding, translation of the information, and response organisation. According to the author's, each stage of information processing may be particularly sensitive to specific experimental variables or factors. RT is affected by different stages of stimulus processing and the interactions of these stages. For instance, the duration of a stage is considered to have an impact on RT. Based on the descriptions of the processing stages in the Additive Factor Model, these processing stages could be linked to particular ERP components: The P1 and the N1 could represent the stimulus encoding stage, as they are known to be modulated by selective spatial attention (Hillyard and Anllo-Vento 1998; Johannes et al. 1995; Luck et al. 1990; Mangun and Hillyard 1991; Störmer et al. 2009). In line with existing literature, in the present visuospatial and non-spatial judgment experiment, P1-MS 2 was modulated by spatial attention and enhanced in more difficult tasks (in the Angle task compared to the Color task).

In the Additive Factor Model (Sternberg 1969), a translation stage may be assigned to P3. Furthemore, a response organisation stage could be also represented by P3. The P3 component is known to reflect a process in between stimulus processing and response planning (Verleger et al. 2005), thus it would seem logical to assign it to these two stages. In our experiments, P3 differed between the conditions depending on the task or the side of stimulation: in

visuospatial and non-spatial judgment, different P3-microstate activation was observed between the two tasks; in the *CRT* task, a higher P3-microstate activity (amplitude) was observed in conditions with a shorter RT.

5.7. Hemispheric asymmetry

In the *CRT* experiment, a stronger activation of the left hemisphere was observed. However, the opposite findings were expected, since the dominance of the right hemisphere in visuospatial information processing was reported in different previous SRT and CRT studies (Nobre et al. 1997; Tuch et al. 2005) and other studies with lateralized visual stimulation (Sheremata et al. 2010; Stephan et al. 2003; Whitford et al. 2011). The right visual field/left hemisphere stimulation evoked stronger activation in N1 and P3 periods. RTs were the shortest for the right visual hemifield/left hemisphere stimulation. Hence, this finding points to the left hemisphere dominance during the execution of the 4-CRT task with lateralized stimulation.

In the visuospatial and non-spatial judgment experiment, the stronger right hemisphere activation was observed in the P1 and N1 time period, and stronger gradients were observed over the right parietal cortex supporting the right hemisphere dominance in visuospatial processing. These findings are in line with existing literature which reports the right hemisphere dominance in visuospatial perception (Colby and Goldberg 1999, Mesulam 1999; Sack et al. 2002b).

5.8. Generalization

This study aimed to investigate the temporal dynamics of visuospatial processing using the EEG microstate method. Two tasks were applied: a 4-CRT task with lateralized stimulation and a visuospatial and non-spatial judgment task. EEG microstate analysis successfully detected differences of

temporal dynamics of networks activation in visuospatial processing steps in both the experiments: that is, between visuospatial (angle) and non-spatial (color) judgment tasks, and for lateralized stimulation. Behavioural data analysis revealed that RT was longer in visuospatial rather than in non-spatial judgment. Also, RT was longer for left visual side stimulation compared to right visual side stimulation, and for medial compared to lateral stimulation in both visual fields. The microstate analysis revealed that visuospatial judgment evoked longer and stronger P1-related activity, and P3-related activity differed in onset, duration and activation between visuospatial and non-spatial judgment. Lateralized stimulation evoked lateralized activation-related N1, and this activation was stronger for right medial stimulation.

Therefore, the visuospatial and non-spatial judgment task and the *4-CRT* task are suitable for use in EEG studies and could be used to develop screening procedures for visuospatial impairment.

6. Conclusions

1. P1-related activity lasts longer and is stronger during visuospatial judgment task than during non-spatial color judgment task.

2. P3-related positivity maximum over the parietal cortex lasts significantly longer and is stronger during non-spatial as compared to visuospatial judgment task.

3. P3-related positivity maximum over the parietal cortex shifts faster from parietal to more central location during visuospatial as compared to non-spatial judgment task.

4. Lateralized visual stimulation evokes early lateralized N1-associated activation that is the strongest for right medial stimulation.

7. References

1. Aglioti S, Berlucchi G, Pallini R, Rossi GF, Tassinari G (1993) Hemispheric control of unilateral and bilateral responses to lateralized light stimuli after callosotomy and in callosal agenesis. Exp Brain Res 95(1):151–165
2. Amunts K, Jäncke L, Mohlberg H, Steinmetz H, Zilles K (2000). Interhemispheric asymmetry of the human motor cortex related to handedness and gender. Neuropsychologia 38(3):304–312
3. Annett M, Annett J (1979) Individual differences in right and left reaction time. Br J Psychol 70(3):393–404
4. Arnáiz E, Almkvist O (2003) Neuropsychological features of mild cognitive impairment and preclinical Alzheimer's disease. Acta Neurol Scand Suppl 179:34–41
5. Barnhardt C, Borsting E, Deland P, Pham N, Vu T (2005) Relationship between visual-motor integration and spatial organisation of written language and math. Optom Vis Sci 82(2):138–143
6. Barthelemy S, Boulinguez P (2001) Manual reaction time asymmetries in human subjects: The role of movement planning and attention. Neurosci Lett 315(1-2):41–44
7. Bartolomeo P, Chokron S (1999) Left unilateral neglect or right hyperattention? Neurology 53(9):2023–2027
8. Basso D, Vecchi T, Kabiri LA, Baschenis I, Boggiani E, Bisiacchi PS (2006) Handedness effects on interhemispheric transfer time: A TMS study. Brain Res Bull 70(3):228–232
9. Battelli L, Cavanagh P, Martini P, Barton JJS (2003) Bilateral deficits of transient visual attention in right parietal patients. Brain 126(Pt 10):2164–2174
10. Benton A, Hannay HJ, Varney NR (1975) Visual perception of line direction in patients with unilateral brain disease. Neurology 25(10):907–910

11. Benton AL, Varney NR, Hamsher KD (1978) Visuospatial judgment. A clinical test. Arch Neurol 35(6):364–367
12. Benwell CSY, Harvey M, Thut G (2014) On the neural origin of pseudoneglect: EEG-correlates of shifts in line bisection performance with manipulation of line length. NeuroImage 86(100): 370–380
13. Bestelmeyer PEG, Carey DP (2004) Processing biases towards the preferred hand: valid and invalid cueing of left- versus right-hand movements. Neuropsychologia 42(9):1162–1167
14. Bilder RM, Wu H, Bogerts B, Degreef G, Ashtari M, Alvir JM, Snyder PJ, Lieberman JA (1994) Absence of regional hemispheric volume asymmetries in first-episode schizophrenia. Am J Psychiatry 151(10):1437–1447
15. Bisiacchi P, Marzi CA, Nikoletti R, Carena G, Musignat C, Tomaiuolo F (1994) Left-right asymmetry of callosal transfer in normal human subjects. Behav Brain Res 64(1-2):173–178
16. Bocci T, Pietrasanta M, Caleo M, Sartucci F (2014) Visual callosal connections: role in visual processing in healthy and disease. Rev Neurosci 25(1):113–127
17. Brandeis D, Lehmann D (1986) Event-related potentials of the brain and cognitive processes: Approches and applications. Neuropsychologia 24(1):151–168
18. Brunet D, Murray MM, Michel CM (2011) Spatiotemporal analysis of multichannel EEG: CARTOOL. Comput Intell Neurosci 2011: 813870. doi: 10.1155/2011/813870
19. Büchel C, Raedler T, Sommer M, Sach M, Weiller C, Koch MA (2004) White matter asymmetry in the human brain: A diffusion tensor MRI study. Cereb Cortex 14(9):945–951
20. Butler PD, Martinez A, Foxe JJ, Kim D, Zemon V, Silipo G, Mahoney J, Shpaner M, Jalbrzikowski M, Javitt DC (2007) Subcortical visual dysfunction in schizophrenia drives secondary cortical impairments. Brain 130(Pt 2):417–430

21. Catani M, Jones DK, Donato R, Ffytche DH (2003) Occipito-temporal connections in the human brain. Brain 126(Pt 9):2093–2107
22. Colby CL, Goldberg ME (1999) Space and attention in parietal cortex. Annu Rev Neurosci 22(1):319–349
23. Coles MGH, Rugg MD (1996) Event-related brain potentials: An introduction. In: Electrophysiology of Mind: Event-Related Brain Potentials and Cognition (Rugg MD, Coles MGH, eds), pp 1–27. New York, NY, US: Oxford University Press
24. Corballis MC (2014) Left brain, right brain: Facts and fantasies. PLoS Biol 12(1). e1001767.doi:10.1371/journal.pbio.1001767
25. Corballis PM, Funnell MG, Gazzaniga MS (1999) A dissociation between spatial and identity matching in callosotomy patients. NeuroReport 10(10):2183–2187
26. Corballis PM, Funnell MG, Gazzaniga MS (2002) Hemispheric asymmetries for simple visual judgment in the split brain. Neuropsychologia 40(4):401–410
27. Corballis PM (2003) Visuospatial processing and the right-hemisphere interpreter. Brain Cogn 53(2):171–176
28. Creem SH, Proffitt DR (2001) Defining the cortical visual systems: “What”, “Where”, and “How”. Acta Psychol (Amst.) 107(1-3):43–68
29. Crow TJ, Chance SA, Priddle TH, Radua J, James AC (2013) Laterality interacts with sex across schizophrenia/bipolarity continuum: An interpretation of meta-analyses of structural MRI. Psychiatry Res 210(3):1232–1244
30. Culham JC, Kanwisher NG (2001) Neuroimaging of cognitive functions in human parietal cortex. Curr Opin Neurobiol 11(2):157–163
31. Daly CJ, Kelley GT, Krauss A (2003) Relationship between visual-motor integration and handwriting skills of children in kindergarten: A modified replication study. Am J Occup Ther 57(4):459–462

32. de Graaf TA, Jacobs C, Roebroeck A, Sack AT (2009) FMRI effective connectivity and TMS chronometry: complementary accounts of causality in the visuospatial judgment network. PLoS ONE 4(12):1–11
33. de Graaf TA, Roebroeck A, Goebel R, Sack AT (2010) Brain network dynamics underlying visuospatial judgment: an FMRI connectivity study. J Cogn Neurosci 22(9):2012–2026
34. Dierks T, Linden DE, Hertel A, Günther T, Lanfermann H, Niesen A, Frölich L, Zanella FE, Hör G, Goebel R, Maurer K (1999) Multimodal imaging of residual function and compensatory resource allocation in cortical atrophy: a case study of parietal lobe function in a patient with Huntington's disease. Psychiatry Res 90(1):67–75
35. Di Russo F, Martínez A, Sereno MI, Pitzalis S, Hillyard SA (2002) Cortical sources of the early visual evoked potentials. Hum Brain Mapp 15(2):95–111
36. Donchin E (1981) Presidential address, 1980. Surprise! ... Surprise? Psychophysiology 18(5):493–513
37. Donchin E, Coles MGH (1988) Is the P300 component a manifestation of context updating? Behav Brain Sci 11(3):357–374
38. Donders FC (1969) On the speed of mental processes. Acta Psychol (Amst.) 30:412–431
39. Dykiert D, Der G, Starr JM, Deary IJ (2012) Age differences in intra-individual variability in simple and choice reaction time: Systematic review and meta-analysis. PLoS One 7(10):e45759. doi: 10.1371/journal.pone.0045759
40. Fallgatter AJ, Brandeis D, Strik WK (1997) A robust assessment of the NoGo-anteriorisation of P300 microstates in a cued Continuosu Performance Test. Brain Topogr 9(4):295–302
41. Fink GR, Dolan RJ, Halligan PW, Marshall JC, Frith CD (1997) Space-based and object-based visual attention: shared and specific neural domains. Brain 120(Pt 11):2013–2028

42. Fink GR, Marshall JC, Shah NJ, Weiss PH, Halligan PW, Grosse-Ruyken M, Ziemons K, Zilles K, Freund HJ (2000) Line bisection judgment implicate right parietal cortex and cerebellum assessed by fMRI. Neurology 54(6):1324–1331
43. Fink GR, Marshall JC, Weiss PH, Stephan T, Grefkes C, Shah NJ, Zilles K, Dieterich M (2003) Performing allocentric visuospatial judgments with induced distortion of the egocentric reference frame: An fMRI study with clinical implications. NeuroImage 20(3):1505–1517
44. Formisano E, Linden DEJ, Di Salle F, Trojano L, Esposito F, Sack AT, Grossi D, Zanella FE, Goebel R (2002) Tracking the mind's image in the brain I: time-resolved fMRI during visuospatial mental imagery. Neuron 35(1):185–194
45. Foxe JJ, Doniger GM, Javitt DC (2001) Early visual processing deficits in schizophrenia: impaired P1 generation revealed by high-density electrical mapping. NeuroReports 12(17):3815–3820
46. Foxe JJ, McCourt ME, Javitt DC (2003) Right hemisphere control of visuospatial attention: Line-bisection judgments evaluated with high-density electrical mapping and source analysis. NeuroImage 19(3):710–726
47. Frecska E, Symer C, White K, Piscani K, Kulcsar Z (2004) Perceptional and executive deficits of chronic schizophrenic patients in attentional and intentional tasks. Psychiatry Res 126(1):63–75
48. Friedman D (1984) P300 and slow wave: The effects of reaction time quartile. Biol Psychol 18(1):49–71
49. Funnell MG, Corballis PM, Gazzaniga MS (1999) A deficit in perceptual matching in the left hemisphere of a callosotomy patient. Neuropsychologia 37(10):1143–1154
50. Fu S, Fedota JR, Greenwood PM, Parasuraman R (2010) Dissociation of visual C1 and P1 components as a function of attention load: An event-related potential study. Biol Psychol 85(1):171–178

51. Gazzaniga M (2000) Cerebral specialization and interhemispheric communication. Brain 123(Pt 7):1293–1326
52. Gomez Gonzalez CM, Clark VP, Fan S, Luck SJ, Hillyard SA (1994) Sources of attention-sensitive visual event-related potentials. Brain Topogr 7(1):41–51
53. Goodale MA, Milner AD (1992) Separate visual pathways for perception and action. Trends Neurosci 15(1):20–25
54. Han S, Weaver JA, Murray SO, Kang X, Yund EW, Woods DL (2002) Hemispheric asymmetry in global/local processing: Effects of stimulus position and spatial frequency. NeuroImage 17(3):1290–1299
55. Hannay HJ, Varney NR, Benton AL (1976) Visual localization in patients with unilateral brain disease. J Neurol Neurosurg Psychiatry 39(4):307–313
56. Hardoy MC, Carta MG, Catena M, Hardoy MJ, Cadeddu M, Dell'Osso L, Hugdahl K, Carpiniello B (2004) Impairment in visual and spatial perception in schizophrenia and delusional disorder. Psychiatry Res 127(1-2):163–166
57. Haxby JV, Grady CL, Horwitz B, Ungerleider LG, Mishkin M, Carson RE, Herscovitch P, Schapiro MB, Rapoport SI (1991) Dissociation of object and spatial visual processing pathways in human extrastriate cortex. Proc Nat Acad Sci U S A 88(5):1621–1625
58. Heim S, Eulitz C, Elbert T (2003b) Altered hemispheric asymmetry of auditory N100m in adults with developmental dyslexia. Neuroreport 14(3):501–504
59. Heim S, Eulitz C, Elbert T (2003a) Altered hemispheric asymmetry of auditory P100m in dyslexia. Eur J Neurosci 17(8):1715–1722
60. Heinze HJ, Luck SJ, Mangun GR, Hillyard SA (1990) Visual event-related potentials index focused attention within bilateral stimulus arrays. I. Evidence for early selection. Electroencephalogr Clin Neurophysiol 75(6):511–527

61. Herbert MR, Harris GJ, Adrien KT, Ziegler DA, Makris N, Kennedy DN, Lange NT, Chabris CF, Bakardjiev A, Hodgson J, Takeoka M, Tager-Flusberg H, Caviness VS (2002) Abnormal asymmetry in language association cortex in autism. Ann Neurol 52(5):588–596
62. Herbert MR, Ziegler DA, Deutsch K, O'Brien LM, Kennedy DN, Filipek PA, Bakardjiev AI, Hodgson J, Takeoka M, Makris N, Caviness Jr. VS (2005) Brain asymmetries in autism and developmental language disorder: a nested whole-brain analysis. Brain 128(Pt 1):213–226
63. Hilgetag CC, Théoret H, Pascual-Leone A (2001) Enhanced visual spatial attention ipsilateral to rTMS-induced "virtual lesions" of human parietal cortex. Nat Neurosci 4(9):953–957
64. Hillyard SA, Anllo-Vento L (1998) Event-related brain potentials in the study of visual selective attention. Proc Natl Acad Sci U S A 95(3):781–787
65. Hillyard SA, Kutas M (1983) Electrophysiology of cognitive processing. Ann Rev Psychol 34:33–61
66. Hultsch DF, MacDonald SWS, Dixon RA (2002) Variability in reaction time performance of younger and older adults. J Gerontol B Psychol Sci Soc Sci 57(2):101–115
67. Husain M, Nachev P (2007) Space and the parietal cortex. Trends Cogn Sci 11(1):30–36
68. Iacoboni M, Fried I, Zaidel E (1994) Callosal transmission time before and after partial commissurotomy. NeuroReport 5(18):2521–2524
69. Iacoboni M, Zaidel E (1995) Channels of the corpus callosum. Evidence from simple reaction times to lateralized flashes in the normal and the split brain. Brain 118(Pt 3):779–788
70. Ipata A, Girelli M, Miniussi C, Marzi CA (1997) Interhemispheric transfer of visual information in humans: The role of different callosal channels. Arch Ital Biol 135(2):169–182

71. Jenner AR, Rosen GD, Galaburda AM (1999) Neuronal asymmetries in primary visual cortex of dyslexic and nondyslexic brains. Ann Neurol 46(2):189–196
72. Johannes S, Münte TF, Heinze HJ, Mangun GR (1995) Luminance and spatial attention effects on early visual processing. Brain Res Cogn Brain Res 2(3):189–205
73. Kaiser DA (2005) Basic principles of quantative EEG. J Adult Dev 12(2-3):99–104
74. Kalyanshetti SB, Vastrad BC (2013) Effect of handedness on visual, auditory and cutaneous reaction times in normal subjects. Al Ameen J Med Sci 6(3):278–280
75. Kelly SP, O'Connell RG (2013) Internal and external influences on the rate of sensory evidence accumulation in the human brain. J Neurosci 33(50):19434 –19441
76. Kikuchi M, Koenig T, Munesue T, Hanaoka A, Strik W, et al. (2011) EEG Microstate Analysis in Drug-Naive Patients with Panic Disorder. PLoS ONE 6(7): e22912. doi:10.1371/journal.pone.002291
77. Kochi K, Koenig T, Strik WK, Lehmann D (1996) Event-related potential P300 microstate topography during visual one- and two-dimensional tasks in chronic schizophrenics. Eur Arch Psychiatry Clin Neurosci 246(6):288–296
78. Koenig T, Kottlow M, Stein M, Melie-García L (2011) Ragu: a free tool for the analysis of EEG and MEG event-related scalp field data using global randomization statistics. Comput Intell Neurosci 2011: doi:10.1155/2011/938925
79. Koenig T, Lehmann D, Merlo MC, Kochi K, Hell D, Koukkou M (1999) A deviant EEG brain microstate in acute, neuroleptic-naive schizophrenics at rest. Eur Arch Psychiatry Clin Neurosci 249(4):205–211
80. Koenig T, Melie-García L (2009) Statistical analysis of multichannel scalp field data. In: Electrical Neuroimaging (Michel CM, Koenig T,

Brandeis D, Gianotti LRR, Wackermann J, eds), pp 169–189. New York: Cambridge University Press

81. Koenig T, Melie-García L (2010) A method to determine the presence of averaged event-related fields using randomization tests. Brain Topogr 23(3):233–242
82. Koenig T, Pascual-Marqui RD (2009) Multichannel frequency and time-frequency analysis. In: Electrical Neuroimaging (Michel CM, Koenig T, Brandeis D, Gianotti LRR, Wackermann J, eds), pp 145–168. New York: Cambridge University Press
83. Koenig T, Stein M, Grieder M, Kottlow M (2014) A tutorial on data-driven methods for statistically assessing ERP topographies. Brain Topogr 27(1):72–83
84. Kolev V, Falkenstein M, Yordanova J (2006) Motor-response generation as a source of aging-related behavioural slowing in choice-reaction task. Neurobiol Aging 27(11):1719–1730
85. Konrad A, Vucurevic G, Musso F, Stoeter P, Winterer G (2009) Correlation of brain white matter diffusion anisotropy and mean diffusivity with reaction time in an oddball task. Neuropsychobiology 60(2):55–66
86. Kravitz DJ, Saleem KS, Baker CI, Mishkin M (2011) A neural framework for visuospatial processing. Nat Rev Neurosci 12(4):217–230
87. Lehmann C, Vannini P, Wahlund LO, Almkvist O, Dierks T (2006) Increased sensitivity in mapping task demand in visuospatial processing using reaction-time-dependent hemodynamic response predictors in rapid event-related fMRI. NeuroImage 31(2):505–512
88. Lehmann D, Faber PL, Galderisi S, Herrmann WM, Kinoshita T, Koukkou M, Mucci A, Pascual-Marqui RD, Saito N, Wackermann J, Winterer G, Koenig T (2005) EEG microstate duration and syntax in acute, medication-naive, first-episode schizophrenia: A multi-center study. Psychiatry Res 138(2):141–156

89. Lehmann D, Ozaki H, Pal I (1987) EEG alpha map series: brain micro-states by space oriented adaptive segmentation. Electroencephalogr Clin Neurophysiol 67(3):271–288
90. Lehmann D, Skrandies W (1980) Reference-free identification of components of checkerboard-evoked multichannel potential fields. Electroencephalogr Clin Neurophysiol 48(6):609–621
91. Lehmann D, Strik WK, Henggeler B, Koenig T, Koukkou M (1998) Brain electric microstates and momentary conscious mind states as building blocks of spontaneous thinking: I. Visual imagery and abstract thoughts. Int J Psychophysiol 29(1):1–11
92. Lindgren SD, Benton AL (1980) Developmental patterns of visuospatial judgment. J Pediatr Psychol 5(2):217–225
93. Lo YC, Soong WT, Gau SSF, Wu YY, Lai MC, Yeh FC, Chiang WY, Kuo LW, Jaw FS, Tseng WY (2011) The loss of asymmetry and reduced interhemispheric connectivity in adolescents with autism: A study using diffusion spectrum imaging tractography. Psychiatry Res 192(1):60–66
94. Løberg EM, Hugdahl K, Green MF (1999) Hemispheric asymmetry in schizophrenia: A “Dual deficits” model. Biol Psychiatry 45(1):76–81
95. Liu Z, Zhang N, Chen W, He B (2009) Mapping the bilateral visual integration by EEG and fMRI. NeuroImage 46(4):989–997
96. Luck SJ, Heinze HJ, Mangun GR, Hillyard SA (1990) Visual event-related potentials index focused attention within bilateral stimulus arrays. II. Functional dissociation of P1 and N1 components. Electroencephalogr Clin Neurophysiol 75(6): 528–542
97. Madden DJ, Whiting WL, Huettel SA, White LE, MacFall JR, Provenzale JM (2004) Diffusion tensor imaging of adult age differences in cerebral white matter: relation to response time. NeuroImage 21(3):1174–1181
98. Madsen KS, Baaré WFC, Skimminge A, Vestergaard M, Siebner HR, Jernigan TL (2011) Brain microstructural correlates of visuospatial choice reaction time in children. NeuroImage 58(4):1090–1100

99. Mangun GR, Hillyard SA (1991) Modulations of sensory-evoked brain potentials indicate changes in perceptual processing during visual-spatial priming. J Exp Psychol Hum Percept Performe 17(4);1057–1074
100. Marshall JC, Fink GR (2001) Spatial cognition: where we were and where we are. NeuroImage 14(1):2–7
101. Marzi CA (1999) The Poffenberger paradigm: A first, simple, behavioural tool to study interhemispheric transmission in humans. Brain Res Bull 50(5-6):421–422
102. Marzi CA, Bisiacchi P, Nicoletti R (1991) Is interhemispheric transfer of visuomotor information asymmetric? Evidence from a meta-analysis. Neuropsychologia 29(12):1163–1177
103. Marzi CA, Grabowska A, Tressoldi P, Bisiacchi PS (1988) Left hemisphere superiority for visuospatial functions in left-handers. Behav Brain Res 30(2):183–192
104. Masure MC, Benton AL (1983) Visuospatial performance in left-handed patients with unilateral brain lesions. Neuropsychologia 21(2):179–181
105. Matsuda Y, Matsui M, Tonoya Y, Ebihara N, Kurachi M (2011) Useful visual field in patients with schizophrenia: a choice reaction time study. Percept Mot Skills 112(2):369–381
106. McCourt ME, Shpaner M, Javitt DC, Foxe JJ (2008) Hemispheric asymmetry and callosal integration of visuospatial attention in schizophrenia: A tachistoscopic line bisection study. Schizophr Res 102(1-3):189–196
107. McIntosh AR, Grady CL, Ungerleider LG, Haxby JV, Rapoport SI, Horwitz B (1994) Network analysis of cortical visual pathways mapped with PET. J Neurosci 14(2):655–666
108. Mesulam MM (1981) A cortical networks for directed attention and unilateral neglect. Ann Neurol 10(4):309–325
109. Mesulam MM (1999) Spatial attention and neglect: parietal, frontal and cingulate contributions to the mental representation and attentional

targeting of salient extrapersonal events. Neuropsychology 354(1387):1325–1346

110. Michel CM, Henggeler B, Lehmann D (1992) 42-channel potential map series to visual contrast and stereo stimuli: Perceptual and cognitive event-related segments. Int J Psychophysiol 12(2):133–145
111. Michel CM, Koenig T, Brandeis D (2009) Electrical neuroimaging in the time domain. In: Electrical Neuroimaging (Michel CM, Koenig T, Brandeis D, Gianotti LRR, Wackermann J, eds), pp 169–189. New York: Cambridge University Press
112. Mishkin M, Ungerleider LG, Macko KA (1983) Object vision and spatial vision: Two cortical pathways. Trends Neurosci 6:414–417
113. Mohr E, Brouwers P, Claus JJ, Mann UM, Fedio P, Chase TN (1991) Visuospatial cognition in Huntington's disease. Mov Disord 6(2):127–132
114. Mooshagian E, Iacoboni M, Zaidel E (2008) The role of task history in simple reaction time to lateralized light flashes. Neuropsychologia 46(2):659–664
115. Mooshagian E, Iacoboni M, Zaidel E (2009) Spatial attention and interhemispheric visuomotor integration in the absence of the corpus callosum. Neuropsychologia 47(3):933–937
116. Murray MM, Brunet D, Michel CM (2008) Topographic ERP analyses: A step-by-step tutorial review. Brain Topogr 20(4):249–264
117. Murray MM, Foxe JJ, Higgins BA, Javitt DC, Schroeder CE (2001) Visuo-spatial neural response interactions in early cortical processing during a simple reaction time task: a high-density electrical mapping study. Neuropsychologia 39(8):828–844
118. Müri RM, Bühler R, Heinemann D, Mosimann UP, Felblinger J, Schlaepfer TE, Hess CW (2002) Hemispheric asymmetry in visuospatial attention assessed with transcranial magnetic stimulation. Exp Brain Res 143(4):426–430

119. Musso F, Brinkmeyer J, Mobascher A, Warbrick T, Winterer G (2010) Spontaneous brain activity and EEG microstates: A novel EEG/fMRI analysis approach to explore resting-state networks. NeuroImage 52(4):1149–1161
120. Newcombe F, Ratcliff G, Damasio H (1987) Dissociable visual and spatial impairments following right posterior cerebral lesions: clinical, neuropsychological and anatomical evidence. Neuropsychologia 25(1B):149–161
121. Ng VWK, Eslinger PJ, Williams SCR, Brammer MJ, Bullmore ET, Andrew CM, Suckling J, Morris RG, Benton AL (2000) Hemispheric preference in visuospatial processing: A complementary approach with fMRI and lesion studies. Hum Brain Mapp 10(2):80–86
122. Nicolas S (1997) On the speed of different senses and nerve transmission by Hirsch (1862). Psychol Res 59(4):261–268
123. Nielsen JA, Zielinski BA, Ferguson MA, Lainhart JE, Anderson JS (2013) An evaluation of the left-brain vs. right-brain hypothesis with resting state functional connectivity magnetic resonance imaging. PLoS ONE 8(8). e71275. doi:10.1371/journal.pone.0071275
124. Nobre AC, Sebestyen GN, Gitelman DR, Mesulam MM, Frackowiak RSJ, Frith CD (1997) Functional localization of the system for visuospatial attention using positron emission tomography. Brain 120(Pt 3):515–533
125. Nobre AC, Sebestyen GN, Miniussi C (2000) The dynamics of shifting visuospatial attention revealed by event-related potentials. Neuropsychologia 38(7):964–974
126. Ocklenburg S, Güntürkün O (2012) Hemispheric asymmetry: The comparative view. Front Psychol 3(5): doi: 10.3389/fpsyg.2012.00005
127. O'Connell RG, Dockree PM, Kelly SP (2012) A supramodal accumulation-to-bound signal that determines perceptual decisions in humans. Nat Neurosci 15(12):1729–1735. doi:10.1038/nn.3248

128. Oka S, van Tonder G, Ejima Y (2001) A VEP study on visual processing of figural geometry. Vision Res 41(28):3791–3803
129. Olejniczak P (2006) Neurophysiologic basis of EEG. J Clin Neurophysiol 23(3):186–189
130. Oldfield RC (1971) The assessment and analysis of handedness: The Edinburg inventory. Neuropsychologia 9(1):97–113
131. Pascual-Marqui RD, Michel CM, Lehmann D (1995) Segmentation of brain electrical activity into microstates: model estimation and validation. IEEE Trans Biomed Eng 42(7):658–665
132. Penhune VB, Zatorre RJ, MacDonald JD, Evans AC (1996) Interhemispheric anatomical differences in Human primary auditory cortex: Probabilistic mapping and volume measurement from magnetic resonance scans. Cereb Cortex 6(5):66l–672
133. Poffenberger AT (1912) Reaction time to retinal stimulation with special reference to the time lost in conduction through nervous centers. Arch Psychol 23:1–73
134. Polich J (2007) Updating P300: an integrative theory of P3a and P3b. Clin Neurophysiol 118(10):2128–2148
135. Posner MI (1980) Orienting of attention. Q J Exp Psychol 32(1):3–25
136. Prvulovic D, Hubl D, Sack AT, Melillo L, Maurer K, Frölich L, Lanfermann H, Zanella FE, Goebel R, Linden DEJ, Dierks T (2002) Functional imaging of visuospatial processing in Alzheimer's disease. NeuroImage 17(3):1403–1414
137. Ramchurn A, de Fockert JW, Mason L, Darling S, Bunce D (2014) Intraindividual reaction time variability affects P300 amplitude rather than latency. Front Hum Neurosci 8:1–9. doi: 10.3389/fnhum.2014.00557
138. Reuter-Lorenz PA, Posner MI (1990) Components of neglect from right-hemisphere damage: An analysis of line bisection. Neuropsychologia 28(4):327–333
139. Ribolsi M, Lisi G, Di Lorenzo G, Koch G, Oliveri M, Magni V, Pezzarossa B, Saya A, Rociola G, Rubino IA, Niolu C, Siracusano A

(2013) Perceptual pseudoneglect in schizophrenia: Candidate endophenotype and the role of the right parietal cortex. Schizophr Bull 39(3):601–607

140. Ringo JL, Doty RW, Demeter S, Simard PY (1994) Time is of the essence: A conjecture that hemispheric specialization arises from interhemispheric conduction delay. Cereb Cortex 4(4):331–343
141. Rizzolatti G, Matelli M (2003) Two different streams form the dorsal visual system: Anatomy and functions. Exp Brain Res 153(2):146–157
142. Rogers LJ, Zucca P, Vallortigara G (2004) Advantages of having a lateralized brain. Proc Biol Sci 271:S420–S422
143. Roser ME, Fiser J, Aslin RN, Gazzaniga MS (2011) Right hemisphere dominance in visual statistical learning. J Cogn Neurosci 23(5):1088–1099
144. Roth WT, Ford JM, Kopell BS (1978) Long-latency evoked potentials and reaction time. Psychophysiology 15(1):17–23
145. Sack AT, Camprodon JA, Pascual-Leone A, Goebel R (2005) The dynamics of interhemispheric compensatory processes in mental imagery. Science 308(5722):702–704
146. Sack AT, Hubl D, Prvulovic D, Formisano E, Jandl M, Zanella FE, Maurer K, Goebel R, Dierks T, Linden DEJ (2002a) The experimental combination of rTMS and fMRI reveals the functional relevance of parietal cortex for visuospatial functions. Cogn Brain Res 13(1):85–93
147. Sack AT, Kohler A, Bestmann S, Linden DEJ, Dechent P, Goebel R, Baudewig J (2007) Imaging the brain activity changes underlying impaired visuospatial judgments: simultaneous fMRI, TMS, and behavioral studies. Cereb Cortex 17(12):2841–2852
148. Sack AT, Sperling JM, Prvulovic D, Formisano E, Goebel R, Di Salle F, Dierks T, Linden DEJ (2002b) Tracking the mind's image in the brain II: Transcranial magnetic stimulation reveals parietal asymmetry in visuospatial imagery. Neuron 35(1):195–204

149. Salvador R, Suckling J, Schwarzbauer C, Bullmore E (2005) Undirected graphs of frequency-dependent functional connectivity in whole brain networks. Phil Trans R Soc 360 (1457):937–946
150. Saron CD, Davidson RJ (1989) Visual evoked potential measures of interhemispheric transfer time in humans. Behav Neurosci 103(5):1115–1138
151. Saville CWN, Dean RO, Daley D, Intriligator J, Boehm S, Feige B, Klein C (2011) Electrocortical correlates of intra-subject variability in reaction time: Average and single-trial analyses. Biol Psychol 87(1):74–83
152. Schechter I, Butler PD, Zemon VM, Revheim N, Saperstein AM, Jalbrzikowski M, Pasternak R, Silipo G, Javitt DC (2005) Impairments in generation of early-stage transient visual evoked potentials to magno- and parvocellular-selective stimuli in schizophrenia. Clin Neurophysiol 116(9):2204–2215
153. Schenk T, McIntosh RD (2010) Do we have independent visual streams for perception and action? Cogn Neurosci 1(1):52–62
154. Schicke T, Muckli L, Beer AL, Wibral M, Singer W, Goebel R, Rösler F, Röder B (2006) Tight covariation of BOLD signal changes and slow ERPs in the parietal cortex in a parametric spatial imagery task with haptic acquisition. Eur J Neurosci 23(7):1910–1918
155. Schlutter ND, Rushworth MFS, Passingham RE, Mills KR (1998) Temporary interference in human lateral premotor cortex suggests dominance for the selection of movements. Brain 121(Pt 5):785–799
156. Sharma T, Lancaster E, Sigmundsson T, Lewis S, Takei N, Gurling H, Barta P, Pearlson G, Murray R (1999) Lack of normal pattern of cerebral asymmetry in familial schizophrenic patients and their relatives – The Maudsley Family Study. Schizophr Res 40(2):111–120
157. Shelton J, Kumar GP (2010) Comparison between auditory and visual simple reaction times. Neurosci Med 1:30–32
158. Shen L, Hu X, Yacoub E, Ugurbil K (1999) Neural correlates of visual form and visual spatial processing. Hum Brain Mapp 8(1):60–71

159. Sheremata SL, Bettencourt KC, Somers DC (2010) Hemispheric Asymmetry in Visuotopic Posterior Parietal Cortex Emerges with Visual Short-Term Memory Load. J Neurosci 30(38):12581–12588
160. Shulman GL, Pope DLW, Astafiev SV, McAvoy MP, Snyder AZ, Corbetta M (2010) Right hemisphere dominance during spatial selective attention and target detection occurs outside the dorsal frontoparietal network. J Neurosci 30(10):3640–3651
161. Ska B, Poissant A, Joanette Y (1990) Line orientation judgment in normal elderly and subjects with dementia of Alzheimer's type. J Clin Exp Neuropsychol 12(5):695–702
162. Smania N, Martini MC, Gambina G, Tomelleri G, Palamara A, Natale E, Marzi CA (1998) The spatial distribution of visual attention in hemineglect and extinction patients. Brain (Pt 9)121:1759–1770
163. Sperry RW (1968) Hemisphere deconnection and unity in conscious awareness. Am Psychol 23(10):723–733
164. Spironelli C, Penolazzi B, Angrilli A (2008) Dysfunctional hemispheric asymmetry of theta and beta EEG activity during linguistic tasks in developmental dyslexia. Biol Psychol 77(2):123–131
165. Steel C, Hemsley DR, Pickering AD (2002) Distractor cueing effects on choice reaction time and their relationship with schizotypal personality. Br J Clin Psychol 41(Pt 2):143–156
166. Sternberg S (1969) The discovery of processing stages: Extension of Donders' method. Acta Psychol 30:276–315
167. Stephan KE, Fink GR, Marshall JC (2007) Mechanisms of hemispheric specialization: Insights from analyses of connectivity. Neuropsychologia 45(2-4):209–228
168. Stephan KE, Marshall JC, Friston KJ, Rowe JB, Ritzl A, Zilles K, Fink GR (2003) Lateralized cognitive processes and lateralized task control in the human brain. Science 301(5631):384–386

169. Stevens A, Lutzenberger W, Bartels DM, Strik W, Lindern K (1997) Increased duration and altered topography of EEG microstates during cognitive tasks in chronic schizophrenia. Psychiatry Res 15(66):45–57
170. Störmer V, McDonald JJ, Hillyard SA (2009) Cross-modal cueing of attention alters appearance and early cortical processing of visual stimuli. Proc Natl Acad Sci U S A 106(52):22456–22461
171. Strelets V, Faber P, Golikova J, Novototsky-Vlasov V, Koenig T, Gianotti LR, Gruzelier JH, Lehmann D (2003) Chronic schizophrenics with positive symptomatology have shortened EEG microstate duration. Clin Neurophysiol 114(11):2043–2051
172. Suchan B, Jokisch D, Skotara N, Daum I (2007) Evaluation-related frontocentral negativity evoked by correct responses and errors. Behav Brain Res 183(2):206–212
173. Suchan B, Zoppelt D, Daum I (2003) Frontocentral negativity in electroencephalogram reflects motor response evaluation in humans on correct trials. Neurosci Lett 350(2):101–104
174. Sur S, Sinha VK (2009) Event-related potential: An overview. Ind Psychiatry J 18(1):70–73
175. Tamnes CK, Fjell AM, Westley LT, Østby Y, Walhowd KB (2012) Becoming consistent: Developmental reductions in intraindividual variability in reaction time arerelated to white matter integrity. J Neurosci 32(3):972–982
176. Tartaglione A, Benton AL, Cocito L, Bino G, Favale E (1981) Poin localization in patients with unilateral brain damage. J Neurol Neurosurg Psychiatry 44(10):935–941
177. Thiebaut de Schotten M, Dell'Acqua F, Forkel SJ, Simmons A, Vergani F, Murphy DGM, Catani M (2011) A lateralized brain network for visuospatial attention. Nat Neurosci 14(10):1245–1246
178. Thulborn KR, Martin C, Voyvodic JT (2000) Functional MR imaging using a visually guided saccade paradigm for comparing activation

patterns in patients with probable Alzheimer's disease and in cognitively able elderly volunteers. AJNR Am J Neuroradiol 21(3):524–531

179. Toga AW, Thompson PM (2003) Mapping brain asymmetry. Nat Rev Neurosci 4(1):37–48
180. Tommasi L (2009) Mechanisms and functions of brain and behavioural asymmetries. Philos Trans R Soc Lond B Biol Sci 364(1519):855–859
181. Tranel D, Vianna E, Manzel K, Damasio H, Grabowski T (2009) Neuroanatomical correlates of the Benton Facial Recognition Test and Judgment of Line Orientation Test. J Clin Exp Neuropsychol 31(2):219–233
182. Trojano L, Grossi D, Linden DEJ, Formisano E, Hacker H, Zanella FE, Goebel R, Di Salle F (2000) Matching two imagined clocks: the functional anatomy of spatial analysis in the absence of visual stimulation. Cereb Cortex 10(5):473–481
183. Tuch DS, Salat DH, Wisco JJ, Zaleta AK, Havelone ND, Rosas HD (2005) Choice reaction time performance correlates with diffusion anisotropy in white matter pathways supporting visuospatial attention. Proc Natl Acad Sci U S A 102(32):12212–12217
184. Ungerleider LG, Mishkin M (1982) Two cortical visual systems. In: Analysis of visual behaviour (Ingle DJ, Goodale MA, Mansfield RJW, eds), pp 549–586. Cambridge, MA: The MIT Press
185. Vandenberghe R, Geeraerts S, Molenberghs P, Lafosse C, Vandenbulcke M, Peeters K, Peeters R, Van Hecke P, Oban GA (2005) Attentional responses to unattended stimuli in human parietal cortex. Brain 128(Pt 12):2843–2857
186. Vannini P, Almkvist O, Dierks T, Lehmann C, Wahlund LO (2007) Reduced neuronal efficacy in progressive mild cognitive impairment: A prospective fMRI study on visuospatial processing. Psychiatry Res 156(1):43–57
187. Vannini P, Almkvist O, Franck A, Jonsson T, Volpe U, Kristoffersen Wiberg M, Wahlund LO, Dierks T (2004) Task demand modulations of

visuospatial processing measured with functional magnetic resonance imaging. NeuroImage 21(1):58–68

188. Vannini P, Lehmann C, Dierks T, Jann K, Viitanen M, Wahlund LO, Almkvist O (2008) Failure to modulate neural response to increased task demand in mild Alzheimer's disease: fMRI study of visuospatial processing. Neurobiol Dis 31(3):287–297
189. Vaughan HG (1982) The neural origins of human event-related potentials. Ann N Y Acad Scis 388:125–138
190. Verleger R (1997) On the utility of P3 latency as an index of mental chronometry. Psychophysiology 34(2):131–156
191. Verleger R (2008) P3b: Towards some decision about memory. Clin Neurophysiol 119(4):968–970
192. Verleger R, Baur N, Metzner MF, Śmigasiewicz K (2014a) The hard oddball: Effects of difficult response selection on stimulus-related P3 and on response-related negative potentials. Psychophysiology 51(11):1089–1100
193. Verleger R, Jaśkowski P, Wascher E (2005) Evidence for an integrative role of P3b in linking reaction to perception. J Psychophysiol 19(3):165–181
194. Verleger R, Metzner MF, Ouyang G, Śmigasiewicz K, Zhou C (2014b) Testing the stimulus-to-response bridging function of the oddball-P3 by delayed response signalsand residue iteration decomposition (RIDE). NeuroImage 100:271–280
195. Vogel EK, Luck SJ (2000) The visual N1 component as an index of a discrimination process. Psychophysiology 37(2):190–203
196. Waberski TD, Gobbelé R, Lamberty K, Buchner H, Marshall JC, Fink GR (2008) Timing of visuo-spatial information processing: Electrical source imaging related to line bisection judgment. Neuropsychologia 46(5):1201–1210
197. Walhovd KB, Fjell AM (2007) White matter volume predicts reaction time instability. Neuropsychologia 45(10):2277–2284

198. Wascher E, Hoffmann S, Sänger J, Grosjean M (2009) Visuo-spatial processing and the N1 components of the ERP. Psychophysiology 46(6):1270–1277
199. Weintraub S, Mesulam MM (1987) Right cerebral dominance in spatial attention. Further evidence based on ipsilateral neglect. Arch Neurol 44(6):621–625
200. Westerhausen R, Kreuder F, Woerner W, Huster RJ, Smit CM, Schweiger E, Wittling W (2006) Interhemispheric transfer time and structural properties of the corpus callosum. Neurosci Lett 409(2):140–145
201. White T, Hongwanishkul D, Schmidt M (2011) Increased anterior cingulated and temporal lobe activity during visuospatial working memory in children and adolescents with schizophrenia. Schizophr Res 125(0):118–128
202. Whitford TJ, Kubicki M, Ghorashi S, Schneiderman JS, Hawley KJ, McCarley RW, Shenton ME, Spencer KM (2011) Predicting inter-hemispheric transfer time from the diffusion properties of the corpus callosum in healthy individuals and schizophrenia patients: A combined ERP and DTI study. NeuroImage 54(3):2318–2329
203. Woodman GF (2010) A brief introduction to the use of event-related potentials (ERPs) in studies of perception and attention. Atten Percept Psychophys 72(8): doi:10.3758/AAP.72.8.2031
204. Yuan H, Zotev V, Phillips R, Drevets WC, Bodurka J (2012) Spatiotemporal dynamics of the brain at rest – Exploring EEG microstates as electrophysiological signatures of BOLD resting state networks. NeuroImage 60(4):2062–2072
205. Zhou G, Liu P, He J, Dong M, Yang X, Hou B, Von Deneen KM, Qin W, Tian J (2012) Interindividual reaction time variability is related to resting-state network topology: An electroencephalogram study. Neuroscience 202:276–282

8. Publications

Antonova I, Bänninger A, Direks T, Griškova-Bulanova I, Koenig T, Kohler A (2015) Differential recruitment of brain networks during visuospatial and color processing: Evidence from ERP microstates. Neuroscience 305:128-138

Antonova I, van Swam C, Hubl D, Dierks T, Griskova-Bulanova I, Koenig T (2016) Reaction time in a visual 4-choice reaction time task: ERP effects of motor preparation, and hemispheric involvement. Brain Topography, doi: 10.1007/s10548-016-0473-7.

Conference abstracts:

1) Antonova I, van Swam C, Hubl D, Dierks T, Griskova-Bulanova I, Koenig T. 4-choice reaction time task reveals abnormalities in schizophrenia. 10th Annual Meeting Clinical Neuroscience, Bern, Switzerland, 22.01.2015;18-19

2) Antonova I, Baenninger A, Kohler A, Griskova-Bulanova I, Dierks T, Koenig T. Clock task – effect of difficulty: timing, hemispheric specialization and reaction time. 6th Conference of Lithuanian Neuroscience Association, Vilnius, Lithuania, 05.12.2014;21

3) Antonova I, van Swam C, Hubl D, Dierks T, Griskova-Bulanova I, Koenig T. Neurobiological substrates of trial by trial variance of reaction time in a lateralized visual choice task. Resting states and state dependent information processing in health and disease. Proceedings of the Sinergia Monte Verità Conference on Resting States and State Dependent Information Processing in Health and Disease, Ascona, Switzerland, 28.09-01.10.2014;4

4) Antonova I, Baenninger A, Kohler A, Griskova-Bulanova A, Dierks T, Koenig T. Frankfurt clock paradigm vs. Bern clock paradigm: task difficulty effects on visouspatial processing. IPEG 18th Bienniel Conference, Leipzig, Germany, 25-28.09.2014;83

5) Antonova I, van Swam C, Hubl D, Dierks T, Griskova-Bulanova I, Koenig T. Schizophrenic Patients Show Abnormal Co-activation of the Hemisphere Ipsilateral to the Stimulation Side. FENS 9th Forum of Neuroscience, 05-09.07.2014

6) Antonova I, van Swam C, Hubl D, Dierks T, Griskova-Bulanova I, Koenig T. Schizophrenic patients show abnormal early brain activation during lateralized visual stimulation. Neuronus 2014 IBRO and IRUN Neuroscience Forum, 25-27.04.2014;35

7) Antonova I, van Swam C, Hubl D, Dierks T, Griskova-Bulanova I, Koenig T. Schizophrenic Patients Show Abnormal Co-activation of the Left Hemisphere during Left Hemifield Stimulation. SAN/NIHC 2014 Meeting, 30.01.-02.02.2014;83

8) Antonova I, Šoliūnas A, Intaitė M. Perception of two Ambiguous Figures. International scientific-practical conference "Virtual instruments in biomedicine", 11.05.2011;35–38 [Article in Lithuanian]

Poster presentations:

1) Antonova I, van Swam C, Hubl D, Dierks T, Griskova-Bulanova I, Koenig T. 4-choice reaction time task reveals abnormalities in schizophrenia. 10th Annual Meeting Clinical Neuroscience, Bern, Switzerland, 22.01.2015

2) Antonova I, Baenninger A, Kohler A, Griskova-Bulanova I, Dierks T, Koenig T. Clock task – effect of difficulty: timing, hemispheric specialization and reaction time. 6th Conference of Lithuanian Neuroscience Association, Vilnius, Lithuania, 05.12.2014

3) Antonova I, van Swam C, Hubl D, Dierks T, Griskova-Bulanova I, Koenig T. Neurobiological substrates of trial by trial variance of reaction time in a lateralized visual choice task. Resting states and state dependent information processing in health and disease. Proceedings of the Sinergia Monte Verità Conference on Resting States and State Dependent Information Processing in Health and Disease, Ascona, Switzerland, 28.09-01.10.2014

4) Antonova I, Baenninger A, Kohler A, Griskova-Bulanova A, Dierks T, Koenig T. Frankfurt clock paradigm vs. Bern clock paradigm: task difficulty effects on visouspatial processing. IPEG 18th Bienniel Conference, Leipzig, Germany, 25-28.09.2014

5) Antonova I, van Swam C, Hubl D, Dierks T, Griskova-Bulanova I, Koenig T. Schizophrenic Patients Show Abnormal Co-activation of the Hemisphere Ipsilateral to the Stimulation Side. FENS 9th Forum of Neuroscience, 05-09.07.2014

6) Antonova I, van Swam C, Hubl D, Dierks T, Griskova-Bulanova I, Koenig T. Schizophrenic Patients Show Abnormal Co-activation of the Left Hemisphere during Left Hemifield Stimulation. SAN/NIHC 2014 Meeting, 30.01.-02.02.2014

Oral presentations:

1) Antonova I, van Swam C, Hubl D, Dierks T, Griskova-Bulanova I, Koenig T. Schizophrenic patients show abnormal early brain activation during lateralized visual stimulation. Neuronus 2014 IBRO and IRUN Neuroscience Forum, 25-27.04.2014

2) Antonova I, Šoliūnas A, Intaitė M. Perception of two Ambiguous Figures. International scientific-practical conference "Virtual instruments in biomedicine", 11.05.2011 [In Lithuanian]

9. Acknowledgment

I would like to express my sincere gratitude to my scientific supervisor prof. dr. Thomas Koenig, my former supervisor dr. Kastytis Dapšys and my consultant doc. dr. Inga Griškova-Bulanova for their support, guidance and encouragement.

I would like to thank you my colleagues from Vilnius University and Bern University Hospital of Psychiatry. I also would like to thank you dr. Axel Kohler from University of Osnabrück.

I am grateful to all the subjects for agreeing to participate in the experiments.

Last but not least, I am thankful to my friends and family for their understanding and support.

10. Curriculum vitae

Personal data

Ingrida Antonova

+37060474905

ingrida.antonova@gmail.com

Education

2011 – present: PhD studies of Biophysics, Vilnius University, Faculty of Natural Sciences, Department of Neurobiology and Biophysic

2009 – 2011: Master of Science in Biology (Neurobiology), Vilnius University, Faculty of Natural Sciences, Department of Biochemistry and Biophysics

2005 – 2009: Bachelor of Science in Biology, Vilnius University, Faculty of Natural Sciences

Trainings

1) SCIEX Fellowship, Bern University, University Hospital of Psychiatry, Department of Psychiatric Neurophysiology, Switzerland, 2013.11.04 – 2015.05.04

2) The Research Council of Lithuania fellowship for research training for PhD students, Bern University, University Hospital of Psychiatry, Department of Psychiatric Neurophysiology, Switzerland, 2012.12.03 – 2013.03.02

3) ERASMUS Training, Centre for Cognitive Neuroscience, University of Turku, Finland, 2010.03.01 – 07.01

Schools and seminars

1) FENS-SFN summer school "Neurodevelopmental Psychiatric Disorders", Bertinoro, Italy, 2014.06.22-28

2) Summer school IBRO Course in Neuroscience, Riga, Latvia, 2013.08.21-29

3) ECNP seminar (European College of Neuropsychopharmacology seminars), Baltezers, Latvia, 2013.05.15-17

4) Neuroscience summer school "VU-UH 1st Intensive Summer Course in Neuroscience: From Molecules to Behavior", Vilnius, Lithuania, 2011.06.14-15

Work experience

2008 – 2010: Coordinator of administrative affairs, Vilnius University, Faculty of Medicine, Department of Anatomy, Histology, and Anthropology

Scientific interests

Visual processing, EEG, ERP